LIPSS

10th INTERNATIONAL WORKSHOP

Orléans, Val de Loire, France

21-23 September 2022

GREMI

cnrs

UNIVERSITE D'ORLEANS

BOOK OF ABSTRACTS

Online version - Abstracts authorized by the authors

https://lipss10.sciencesconf.org/

Orléans, 21-23 September 2022

FOREWORD

Surface texturing and structuring of materials at the micro and nano scales is an attractive topic for advanced technologies and life applications in a variety of fields including energy harvesting, functional surfaces, medicine, as well as bio and eco-systems. Laser Induced Periodical Surface Structures (LIPSS) at the heart of several projects conducted throughout many European and international institutions and research labs. LIPSS items under various scientific journals databases show a consistently growing trend in surface structuring. Following a hiatus of a couple of years due to the COVID-19 pandemic, we are glad to announce the 10th Int. LIPSS Workshop that aims at welcoming all scientists from the laser community (and those from the ion/electron beams community are also welcomed!) to share recent progress in LIPSS formation and surface structuring mechanisms through experimental and theoretical approaches. With the technical assistance and support of the University of Orléans, the CNRS, and the Studium, Orléans will offer a beautiful and stimulating environment for the success of this workshop.

Following the previous editions in Saint-Etienne (2017), Bochum (2018) and Ljubljana (2019), the tenth LIPSS Workshop in Orléans will be especially devoted to recent progress and studies on mechanisms formation, considering a wide range of materials (polymers, oxides, metal alloys and compounds, carbon hybrid surfaces...) using various laser sources from short to ultra-short beams pulses. The workshop will also tackle various facets of the science and technology of LIPSS, starting with fundamentals and extending to more applied aspects such as large area processing as well as real-life applications and potential implementation in an industrial setting.

This workshop is intended for all researchers, scientists and students working on LIPSS formation in European and international universities, research centers and institutes as well as in the private sector. Attendees will have the opportunity to bring their questions to leaders in the field of laser-matter interaction for material processing. The workshop will take place in person to provide maximum interaction between participants.

The organizing committee of LIPSS10

INTERNATIONAL SCIENTIFIC BOARD

Alexander KOVACEVIC	Serbia
Esther REBOLLAR	Spain
Evgueny GUREVICH	Germany
Florence GARRELIE	France
Gerard O'CONNOR	Ireland
Giorgos TSIBIDIS	Greece
Jean-Philippe COLOMBIER	France
Johannes HEITZ	Austria
John LOPEZ	France
Jörg KRÜGER	Germany
Jörn BONSE	Germany
Juergen REIF	Germany
Klaus ZIMMER	Germany
Malek TABBAL	Lebanon
Nadjib SEMMAR	France
Peter GREGORCIC	Slovenia
Rainer KLING	France
Salvatore AMORUSO	Italy
Stefan GRÄF	Germany
Tatiana ITINA	France
Thibault DERRIEN	Czech Republic
Sedao XXX	France

LOCAL ORGANIZING COMMITTEE

Corinne DELHAYE	GREMI, University of Orléans/CNRS
Maxime MIKIKIAN	GREMI, University of Orléans/CNRS
Hervé RABAT	GREMI, University of Orléans/CNRS
Nadjib SEMMAR	GREMI, University of Orléans/CNRS
Anne-Lise THOMANN	GREMI, University of Orléans/CNRS
Malek TABBAL	American University of Beirut (AUB)
Sedao XXX	LabHC, University Jean-Monnet-CNRS
Olga SHAVDINA	Decor World Service (DWS)
Aurélien MONTAGU	Le Studium

SPONSORS


GREMI


LABORATOIRE
HUBERT CURIEN
UMR • CNRS • 5516 • SAINT-ETIENNE


cnrs


Université
d'ORLÉANS


Centre-
Val de Loire
www.centre-valdeloire.fr


MATEX
MULTIMATÉRIAUX EN CONDITIONS EXTRÊMES


LE STUDIUM
Loire Valley
Institute for Advanced Studies


DWS


Amplitude


OPTON LASER
INTERNATIONAL


OPTOPRIM
LIGHT
CONVERSION

Wednesday, September 21

11:00	Welcome	
12:30	Lunch	
14:00	Welcome talk	**Anne-Lise Thomann** GREMI, Orléans
14:10	Presentation of Le Studium	**Aurélien Montagu & Marie Artiges** Le Studium, Orléans
14:30	Introduction to the LIPSS Workshop	**Jurgen Reif** BTU, Cottbus-Senftenberg
15:00	Formation dynamics of periodic surface patterns in Ge induced by UV nanosecond laser pulses	**Jan Siegel** Instituto de Optica-CSIC, Madrid
15:35	Coffee Break	
15:55	How the combination of electromagnetic effects and thermophysical properties of solids influences the formation of laser induced periodic surface structures	**George Tsibidis** IESL-FORTH, Heraklion
16:30	Bio-inspired laser micro- and nanopatterning for fluid transport and anti-adhesive properties	**Cristina Plamadeala** Johannes Kepler Universität, Linz
17:05	Round table	
17:45	End of working day	
18:00	Visit of old town	

Thusrday, September 22

09:00	LIPSS formation on polymer thin films: influence of thickness, roughness and substrate	**Esther Rebollar** IQFR-CSIC, Madrid
09:35	LIPSS with extreme properties: short period and high aspect ratio	**Evgeny Gurevich** University of Applied Science, Münster
10:10	Coffee Break	
10:30	Surface Morphology at Nanometric Scale by Temporal and Polarization Control of Ultrashort Laser Pulses	**Anthony Nakhoul** Laboratoire Hubert Curien, Saint-Étienne
11:05	Stochasticity versus determinism in LIPSS formation	**Jean Philippe Colombier** Laboratoire Hubert Curien, Saint-Étienne
11:40	Investigation of LIPSS structures fabricated in different surrounding media using focused-ion beam etching	**Matej Senegacnik** Faculty of Mechanical Engineering, Ljubljana
12:15	Lunch	
14:00	Round table	
14:30	Significance of laser processing environments in determining the surface chemistry, ageing and final response of HSFLs generated on Tungsten	**Priya Dominic** Laboratoire Hubert Curien, Saint-Étienne
15:05	Microscopy techniques for in-situ LIPSS detection and characterization via optical means	**Cyril Mauclair** Laboratoire Hubert Curien, Saint-Étienne
15:40	LIPSS nanostructuring by picosecond laser beam of GDC/YSZ oxide thin films	**Wael Karim** GREMI, Orléans
16:15	Coffee Break	
16:35	Sponsors' presentations	**Opton Laser, Amplitude, Optoprim**
17:35	End of working day	
19:00	Gala dinner at Bateau Lavoir	

Friday, September 23

09:00	Mitigation of secondary electron yield by femtosecond pulse laser-induced periodic surface structuring	**Salvatore Amoruso** Complesso Universitario di Monte S. Angel, Napoli
09:35	The influence of LIPSS spatial alignment and periodicity on osteoblastic differentiation	**Xxx Sedao** Laboratoire Hubert Curien, Saint-Étienne
10:10	Coffee Break	
10:30	Industrialization considerations of ultrashort LIPSS texturing for biological applications	**Yoan Di Maio** GIE Manutech-USD, Saint-Étienne
11:05	Smart laser engraving system for wide-band gap materials for the luxury industry	**Alex Capelle** GREMI, Orléans
11:40	Round table	
12:10	Closing session - Conclusions - Next workshop organization	
12:30	Lunch	
14:00	Potential visit: GREMI laboratory and DWS start-up	
17:00	End of working day	

Table of contents

FORMATION DYNAMICS OF PERIODIC SURFACE PATTERNS IN GE INDUCED BY UV NANOSECOND LASER PULSES

M. ALVAREZ-ALEGRIA[1], C. RUIZ DE GALARRETA[1] AND JAN SIEGEL[1]*

[1] Laser Processing Group, Instituto de Óptica, IO-CSIC, Serrano 121, 28006 Madrid, Spain
*j.siegel@csic.es

ABSTRACT

Direct Laser Interference Patterning (DLIP) is a versatile technique that enables the single pulse fabrication of periodic surface structures over relatively large areas in a variety of materials [1],[2]. The sinusoidal shape of the intensity profile cross sections at the sample surface created by two or more interfering laser pulses triggers the formation of periodic surface patterns, whose periodicity can be tuned by modifying the irradiation configuration. In that sense, DLIP can be considered to belong to the larger category of laser induced periodic surface structures (LIPSS) fabrication strategies, with the added benefit of single pulse operation, tunable period, highly homogeneous feature shapes and orientations for a wider range of materials.

In this work, we have employed DLIP to process crystalline Ge using interfering unpolarised UV excimer laser pulses (ArF, $\lambda = 193$ nm, $\tau = 23$ ns). Using single pulse irradiation, homogenous diffraction gratings as large as 0.5 x 0.5 mm can be fabricated. The imprinted fringes are highly periodic and parallel, with a steep height modulation profile across the fringes. In order to unravel the formation dynamics of these periodic structures, we have performed time-resolved optical reflectivity and diffraction measurements with ns temporal resolution, which enable us to follow in real-time the dynamics not only of the melting and solidification process but of the evolution of the surface topography. Combined with a simple model of the diffraction efficiency of these structures, 3D maps of the transient surface elevation as a function of fluence and time can be obtained. The results reveal that the formation process of the 3D structures can be understood when taking into account both, Marangoni effect and the presence of thermocapillary waves with an oscillation period in the range of a few tens of nanoseconds.

REFERENCES

[1] A.I. Aguilar-Morales, S. Alamri, A.F. Lasagni, “Micro-fabrication of high aspect ratio periodic structures on stainless steel by ps direct laser interference patterning”, J. Mater. Process. Technol. 252 313–321 (2018).

[2] I. Martín-Fabiani, S. Riedel, D.R. Rueda, J. Siegel, J. Boneberg, T. a Ezquerra, A. Nogales, “Micro- and Submicrostructuring Thin Polymer Films with Two and Three-Beam Single Pulse Laser Interference Lithography”, Langmuir 30 8973–8979 (2014).

HOW THE COMBINATION OF ELECTROMAGNETIC EFFECTS AND THERMOPHYSICAL PROPERTIES OF SOLIDS INFLUENCES THE FORMATION OF LASER INDUCED PERIODIC SURFACE STRUCTURES

GEORGE D. TSIBIDIS[1,2*] , PANAGIOTIS LINGOS[1] , EMMANUEL STRATAKIS[1,3]

[1]Institute of Electronic Structure and Laser (IESL), Foundation for Research and Technology (FORTH), Vassilika Vouton, 70013, Heraklion, Crete, Greece

[2]Department of Materials Science and Technology, University of Crete, 71003, Heraklion, Greece

[3]Department of Physics, University of Crete, 71003, Heraklion, Greece

*tsibidis@iesl.forth.gr

ABSTRACT

To realize efficient material processing and account for the formation of laser induced periodic surfaces structures (LIPSS), it is very important to understand the fundamental laser-matter interaction processes. In this work, we follow a systematic approach to predict the *pulse-by-pulse* formation of LIPSS on metals due to the development of a spatially periodic energy deposition that results from the interference of electromagnetic far fields on a non-flat surface profile. We demonstrate that the induced electromagnetic effects, alone, are not sufficient to allow the LIPSS formation, therefore, we emphasize on the crucial role of electron diffusion and electron-phonon coupling on the formation of stable periodic structures. Gold and stainless Steel are used as two materials to test the model.

1. INTRODUCTION

The employment of femtosecond (fs) pulsed laser sources for material processing has received significant attention due to the important technological applications [1]. Various types of surface nano/micro-structured topographies have been fabricated by exploiting the wealth of possibilities laser technology offers through modulation of the laser parameters [1,2].

Despite the presence of several theoretical frameworks that aim to elucidate the surface modification related underlying physical processes, it has been postulated that the pattern formation is attributed to a great extent to the response of the solid to the electromagnetic radiation [1,3,4]. However, experimental results for various metals showed that while the size and origin of the periodicity of LIPSS can be ascribed to electromagnetic effects, the manifestation of the depth profile of the produced periodic structures varies [5,6]. Although, one might argue that, the electromagnetic response of the irradiated material (i.e. different extinction coefficient) accounts for this behavior, experimental observations demonstrate that other physical mechanisms can potentially be involved that allow or inhibit the formation of distinct periodic structure.

In this work [4], we demonstrate that the thermophysical properties of the material themselves play a crucial role in the formation of periodic patterns. To this end, we have conducted a multiscale physical modelling approach to describe pattern formation on two materials, gold (Au) and stainless Steel (SS) that are characterized from distinctly different thermophysical properties.

2. THEORETICAL PREDICTIONS

Our theoretical predictions are aimed to reveal the significant role of the differences in the electron

diffusion and electro-phonon coupling strengths in the two materials to the features of the induced topographies. We emphasize the interplay between the electromagnetic and thermophysical properties in the produced amplitude of periodic structures through a detailed theoretical investigation. In our simulations, linearly polarized laser beams of pulse duration 170 fs (FWHM) were used. It is noted that the electric field is polarized along the *X*-axis.

To describe, firstly, the electromagnetic response of the two materials, lightly rough surfaces are assumed. The aim is to show that non-flat topographies account for the excitation of electromagnetic modes that are precursors of periodic structures. To emulate the rough patterns, a configuration of a random distribution of sub-wavelength hemispherical holes (radius randomly ranged between $10< R \quad 100$ nm) is used along the surface. A similar approach has been introduced in previous reports [3].

The interaction of light with the surface inhomogeneities of the material produces electromagnetic interference patterns along the surface which determines the energy absorption landscape. Hence, the investigation of the periodic (or quasi-periodic) electromagnetic modes along the surface is the first step in our multi-physical study. The interference between the incident light beam with the scattered waves generated by surface nano-defects on metallic surfaces as a result of dipole-dipole coupling, produce standing mixed waves such as Surface Plasmon Polaritons (SPP) and quasi-cylindrical evanescent waves [3]. The optical properties of the irradiated material determine the characteristics of these waves such as scattering, absorption, transmission, the optical propagation length as well as the skin depth. To reveal the electromagnetic response of the material, a Finite Integration Technique is employed for the solution of the full-vector 3D Maxwell-Grid Equations [4]. Assuming a laser beam at a fixed wavelength $\lambda_L = 513$ nm, the dielectric constants considered in the simulations are $\varepsilon_{Au} = -3.43 + i3.01$ and $\varepsilon_{SS} = -0.45 + i16.3$ for Au and SS, respectively, whereas the hemispherical nano-holes are assumed to be filled with air ($\varepsilon = 1$).The electric field of the laser beam is presented as a plane-wave linearly polarized along the X-axis arriving at normal incidence to the surface. The geometry of the problem allows to use a simple representation of the boundary conditions and the computational grid is terminated by two convolutional perfectly matched layers (convPML) [4] along the *Z*-direction to avoid non-physical reflections while periodic boundary conditions are used for *X* and *Y* directions.

It is noted that in order to compare the surface deformation of both materials following the multi-pulse irradiation, we used identical surface topographies before the arrival of the initial laser pulse. To acquire information about the energy absorption in these two samples, we illustrated the inhomogeneous distribution of the intensity, $I \sim \left|\vec{E}\right|^2$ (where $\vec{E}$ stands for the electric field), below the rough surface normalized with respect to the maximum intensity of the flat surface I_S or the maximum intensity of the incident beam by the source. In Fig.1a-b, we show the normalized intensity difference $(I - I_S)/I_S$ below the surface in the transverse plane perpendicular to light wave-vector, which depicts the intensity maxima and minima due to both scattered radiative and non-radiative fields by the subwavelength imperfection. It appears, that the presence of the nano-holes in the metallic surfaces favor the energy deposition at their edges, localized parallel to the laser polarization, while the far fields consisting of SPP and quasi-cylindrical wave components exhibit maxima and minima that are formed perpendicularly to the laser polarization. For both metals in the current work, the superposition of the incident beam with the scattered far fields determines the energy absorption maps along the surface. It is noted that there exists a strong difference in the optical properties and response of the materials: (a) the absorption coefficient (b) the SPP propagation length and (c) the skin depth. For instance, the absorption coefficient of is $a_{Au} = 81.73\ \mu\text{m}^{-1}$ and $a_{SS} = 47.75\ \mu\text{m}^{-1}$ for the two materials. The SPP propagation length is $L_{Au} \approx 100\ \mu$m for Au and $L_{SS} = 0.23\ \mu$m for SS. Despite these differences, the absorption features of these materials are quite similar and they are determined by the radiative far fields. On the other hand, the near field couplings are negligible because the average distance between the nano-holes is nearly equal to the laser wavelength. As a result, the periodic/quasi-periodic absorption features are observed with average periodicity $\approx \lambda_L$. This is also captured in Fast Fourier Transforms of the corresponding absorption maps ($k_x/k_0 \approx \pm 1$) (Fig.1c-d). Moreover, the periodic absorption features are strongly defined by the SPP. In Fig.1e-f, we present the normalized *Z*-component of the electric

field at the propagation plane *XZ* which depicts the SPP along the air-metal interface; in the case of Au, the SPP is pronounced compared to the stainless steel. To correlate the

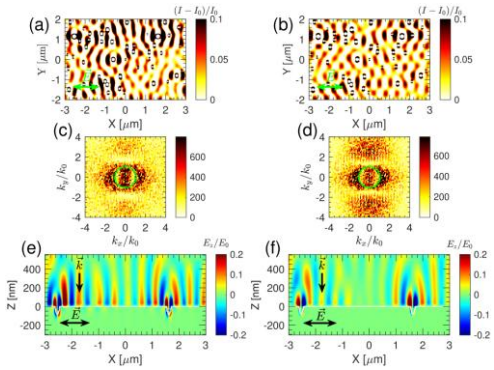

Fig.1. Absorbed energy distributions on the transverse plane for Au (a) and SS (b) surfaces (*NP*=1). (c), (d) illustrate the Fourier transform of (a), (b), respectively. The *green* circles represent the boundary of $|k| = k_0$ where $k_0 = 2\pi/\lambda_L$ stands for the wave-vector of light propagation in air (double headed arrow indicates laser polarization direction). (e) and (f) illustrate normalized *Z*-component of the electric field at the propagation plane *XZ*. In this cross section, two nano-holes are located at positions *X*=-2540 nm and *X*=1630 nm. The *white* line represents the air-metal interface.

electromagnetic response of the material with changes occurring along the irradiated surface in a pulse after pulse approach, a side view of the distribution of the absorbed energy is illustrated for both materials on the *XZ* plane (the propagation plane) for four pulses (*NP*=4) (Fig.2a and Fig.2b); by contrast, results illustrated in Fig.1 are obtained for *NP*=1. The electric field (*Z*-component) distribution on the propagation plane for the two materials is also illustrated in Fig. 2c and Fig.2d. Results for Au and SS demonstrate similar far field interference patterns of the absorbed energy, following scattering of the electromagnetic fields off the hole scatterers. The quasi-periodic interference patterns (Fig.1a,b) induced by nanoscale surface imperfections can explain the formation mechanism of laser-induced patterns [3,4]. Thus, a reasonable outcome of such electromagnetic field distribution would be the formation of periodic structures (LSFL) on the surface of both materials. Nevertheless, experimental results indicate that, unlike in SS, the amplitude of the ripples formed on bulk Au is very small even at very large number of pulses [6]. This outcome suggests that other effects related to the properties of the metals and thermal response of system after absorbing the laser energy might account for the distinct differences.

To describe the process towards pattern formation we use a theoretical model that comprises a Two Temperature Model (TTM) coupled with a Navier-Stokes equation that provides a detailed analysis of the fluid dynamics [2,4]. Due to the large electron heat diffusion and ballistic transport for Au, less energetic electrons remain on the surface of the material to couple with the lattice system. By contrast, the behavior of SS, both in terms of electron diffusion and electron-phonon coupling strength, is different: the electron heat conductivity length is four times smaller than those for Au while the electron phonon coupling strength is ten time stronger and it follows a decreasing monotonicity with increasing electron temperature (opposite to that of Au). As a result, larger lattice temperatures are confined in a smaller region, thus the developed temperature gradients are more enhanced and finally, the induced hydrothermal waves will have larger amplitudes, giving rise to pronounced periodic profiles upon resolidification [4].

To illustrate the effect of repetitive irradiation, we have carried out simulations at increasing *NP*. Results show an enhanced absorption in the wells of the periodic profile (Fig.2). As repetitive irradiation is expected to increase the amplitude of the induced periodic structures due to mass transport, the theoretical framework was applied to predict the variation of the height and periodicity of the ripples (Fig.3). Simulations results for both Au and SS show a shallow ripple profile for Au (Fig.3a), compared to higher ripple amplitudes for SS (Fig.3b) due to the predominantly energy confinement for SS. Although simulations shown in Fig.3 provide results for *NP*=4, similar conclusions can be deduced at higher *NP*. With respect to the periodicity variation at increasing *NP*, it

is noted that results in previous works showed a decrease of the ripple periodicity as *NP* increases [2,3]; by contrast, our simulations indicate that for a small *NP*, an apparent ripple periodicity reduction is not predicted (Fig.3c). Finally,

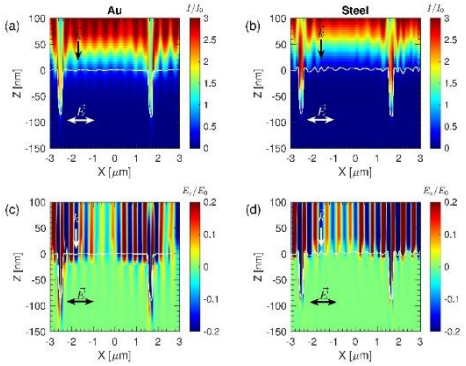

Fig.2. Absorbed energy distributions on the propagation plane for (a) Au and (b) SS surfaces (*NP*=4). Electric field (*Z*-component) distribution for Au (c), SS (d). The *white* line defines the boundary of the surface profile along the air-metal interface.

the expected increase of the amplitude of the produced ripples for SS, in contrast to Au, at increasing *NP* is illustrated in Fig.3d.

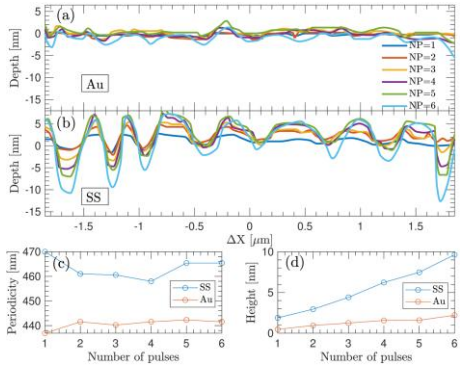

Fig.3. Amplitude of LIPSS as a function of number of pulses for (a) Au and (b) Stainless steel. Average periodicity (c) and (d) amplitude of LIPSS *vs* number of pulses.

3. CONCLUSIONS

Our approach was aimed to interpret the differences in the periodic pattern amplitudes following irradiation of materials with distinctly different thermophysical properties. The investigation (i) predicts the excitation of electromagnetic modes of periodicities of the size of the wavelength, and (ii) demonstrates the significant influence of the electron diffusion and electron-phonon coupling on the features of the expected periodic patterns. While, in the current study, the focus is on the LSFL features on Au and SS, a similar approach could be followed for other materials.

Funding. *BioCombs4Nanofibres* (grant agreement No. 862016); *NEP* project (GA 101007417); COST Action *TUMIEE*.

REFERENCES

[1] E. Stratakis *et al.*, Materials Science and Engineering: R: Reports **141**, 100562 (2020).
[2] G. D. Tsibidis, M. Barberoglou, P. A. Loukakos, E. Stratakis, and C. Fotakis, Physical Review B **86**, 115316 (2012).
[3] A. Rudenko, C. Mauclair, F. Garrelie, R. Stoian, and J. P. Colombier, Applied Surface Science **470**, 228 (2019).
[4] G. Tsibidis, P.Lingos, and E. Stratakis, Optics Letters **47**, 4251 (2022).
[5] J. C. Wang and C. L. Guo, Applied Physics Letters **87**, 251914 (2005).
[6] F. Fraggelakis, G. D. Tsibidis, and E. Stratakis, Physical Review B **103**, 054105 (2021).

BIO-INSPIRED LASER MICRO- AND NANOPATTERNING FOR FLUID TRANSPORT AND ANTI-ADHESIVE PROPERTIES

C. PLAMADEALA[1]*, G. BUCHBERGER[1], J. HEITZ[1], W. BAUMGARTNER[2]

[1]Institute of Applied Physics, Johannes Kepler University Linz, 4040, Linz, Austria
[2]Institute of Biomedical Mechatronics, Johannes Kepler University Linz, 4040, Linz, Austria
*cristina.plamadeala@jku.at

ABSTRACT

Bio-inspired micro- and nano-patterning of materials by means of laser radiation is a rapidly growing field for special industrial, medical, and scientific applications. This is significantly driven by the exciting properties of micro- and nano-patterned materials found in natural biological species, including wetting, directional fluid transport [1] and pronounced adhesive and anti-adhesive properties [2]. The structuring techniques addressed here focus on developments in laser processing using short and ultrashort laser pulses. This includes the self-organized formation of periodic micro- and nano-patterns at surfaces induced by exposure to laser radiation, as well as direct patterning techniques such as two-photon polymerization and UV lithography.

1. INTRODUCTION

Laser-induced periodic surface structures (LIPSS) are self-assembled micro- and nano-structures which can be generated by linearly polarized radiation on most materials. They allow the manipulation of important surface properties. As their fabrication is flexible, robust and mostly fast, LIPSS have found applications in fields of optics, fluidics, electronics, tribology, medicine etc. In this paper, we present an overview of our recent work, shortly covering the topic of bio-inspired LIPSS that can be used in directional fluid transport and adhesive and anti-adhesive surfaces applications.

2. MATERIALS AND METHODS

In this section we describe the setup used to produce all LIPSS presented in this paper, shown in **Fig. 1** and described in more details in [3]. The setup consists of a KrF* excimer laser (LPX 300, former Lambda Physik, now Coherent Deutschland GmbH, Germany), with a wavelength of 248 nm, and a pulse duration of 20 ns. The laser beam is linearly polarized with a α-BBO crystal (Melles Griot, Carlsbad, CA, USA), and projected onto the rotatable sample holder with the help of two fused silica lenses arranged in a telescope configuration. The sample is fixed on the sample holder with adhesive tape, and exposed to the KrF* laser beam under different angles of incidence, θ.

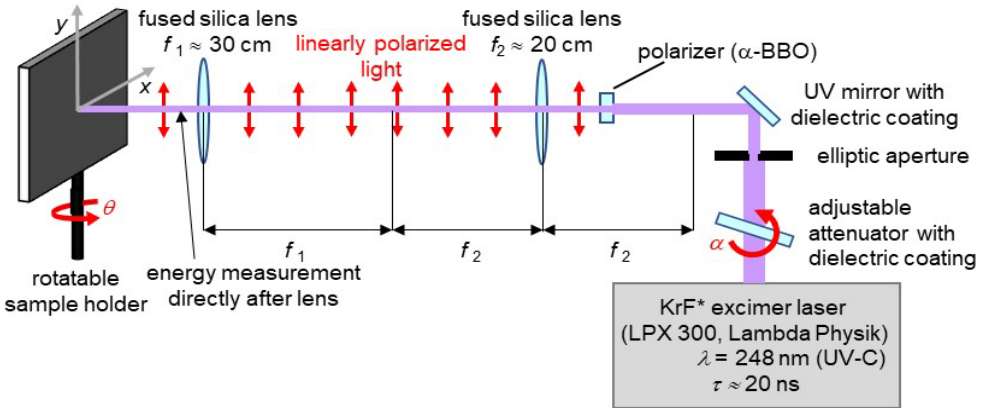

Fig. 1 Setup for LIPSS fabrication on polymer foils [4].

3. LIPSS FOR DIRECTIONAL FLUID TRANSPORT

In a biomimetic approach to imitate the wettability and directional fluid transport of the scent efferent system of true bugs [5], polyimide (PI) foils (UBE Industries, Ltd) were irradiated with the KrF* laser under a 45° incidence angle. This resulted in formation of tilted conical microstructures with a length of 25 µm and a width of 13 µm (**Fig. 2A** and **B**), comparable with the structures in the natural role model. To obtain a longer channel, the PI foil was horizontally moved at a speed of about 16.7 µm/s. The sample was exposed to 400 pulses, at repetition rate of 5 Hz, and with a fluence of 75 mJ/cm².

Wetting tests were performed to assess the wettability and eventual unidirectional fluid transport using a soap-water solution (with a contact angle of 35°, measured on non-processed PI foils) mixed with Ponceau Red dye (Sigma Aldrich, Germany). Samples were fixed at 45°, in such a manner that the tips of the cones point upwards. A 0.4 µL droplet of soap-water solution was applied in the middle of the structured area. It can be seen in **Fig. 2C**, that the liquid solution is moving upwards, against gravity, reaching the upper rim of the structured area, while the liquid front was halted in the downwards direction. These results show that it is possible to obtain an upwards directional liquid transport on a tilted surface, against gravity.

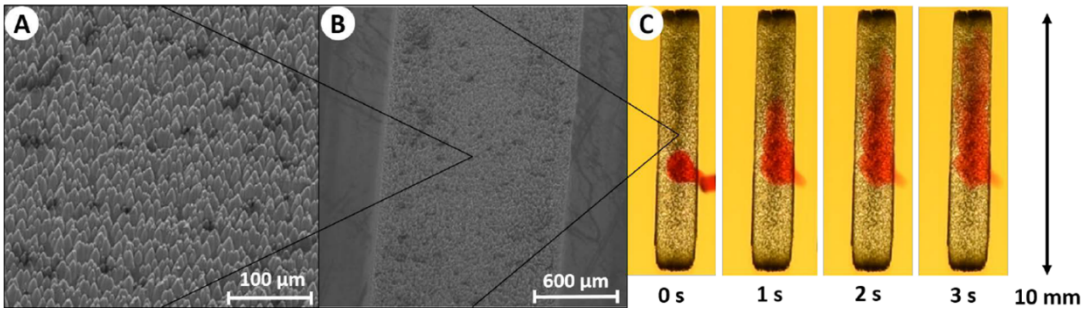

Fig. 2 Polyimide tilted conical structures. (A, B) Scanning electron microscope images (SEM) of the structures within the irradiated surface of the polyimide foil. (C) Directional liquid movement of the soap-water solution with a contact angle of 35° on an irradiated surface area of 10 mm × 1.5 mm, tilted at an angle of 45° starting from liquid deposition (0 s) and ending when the liquid has reached the upper rim of the structured area (3 s) [6].

4. LIPSS FOR ANTI-ADHESION APPLICATIONS

Cribellate spiders employ their *calamistrum* located on their hindmost legs (**Fig. 4A**), to process and assemble nanofibers into structurally complex capture threads [2]. A *calamistrum* (**Fig. 4B**) is a specialized comb, composed of fingerprint-like nanostructures. These structures hinder the nanofibers to adapt to the comb's surface, and therefore, reduce the contact area and the adhesive van der Waals forces between the nanofibers and the surface. Similar structures as found on the *calamistrum* can be produced on poly(ethylene terephthalate) (PET) foils (**Fig. 4C**) with a KrF* laser setup as described earlier. PET foils were irradiated under an incidence angle of 30°, with 6000 pulses, at a fluence of 10 mJ/cm², and a repetition rate of 10 Hz, resulting in a spatial period of the ripples of about 350 nm, and a ripple height of 100 nm.

Adhesion measurements were performed on structured and unstructured samples, as well as on their gold-coated counterparts (this step was performed to reduce the electrostatic forces). The samples were initially bent and brought into contact with the natural fibers, and afterwards - slowly and constantly drawn away from the thread until detachment. The measurements were video-recorded and the deflection of the nanofibers was measured and plotted as shown in **Fig. 4D**. It is clear that the gold-coated structured PET foil deflects the spider fibers the least, making it the least sticky surface. Also, it has been recently shown that the anti-adhesion depends on the ambient temperature and humidity [7]. As a technical application, structured surfaces could be used as collectors in electrospinning setups, making it easier to peel off the nonwoven nanofiber fabric.

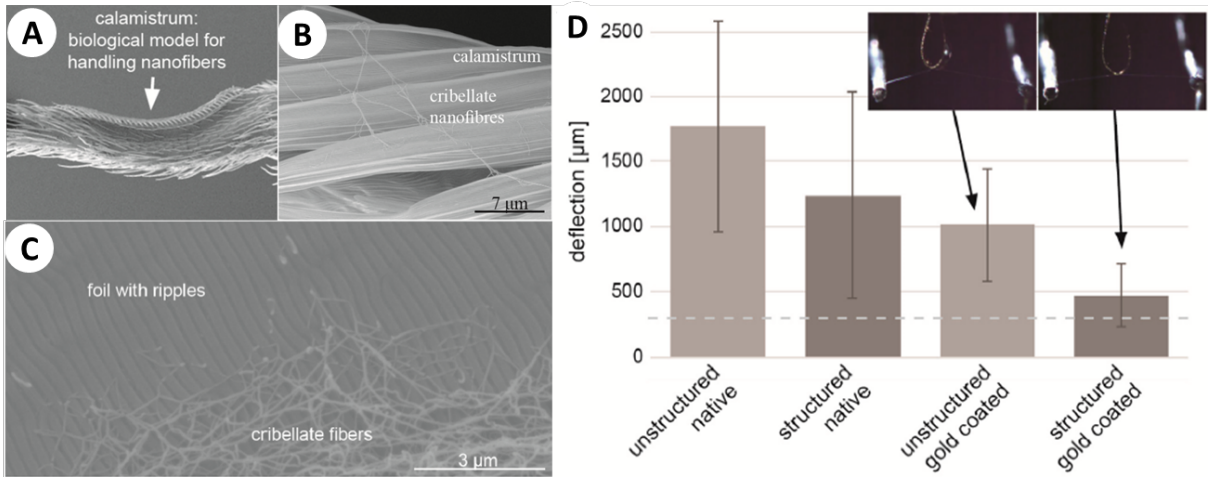

Fig. 3 (A) SEM of the metatarsus of the fourth leg of a cribellate spider, showing the depression where the *calamistrum* is situated as a specialized row of setae. (B) SEM close-up of single cribellate nanofibers placed artificially over the *calamistrum*. (C) Foil with nano-ripples as a biomimetic replication of the *calamistrum*, with artificially placed nanofibers on its surface. (D) Indirect measurement of the adhesive forces between the biomimetic foil by measuring the deflection of a 7-mm-long cribellate thread (insets: maximal deflection of the cribellate thread attached to a gold-coated structured foil and to an unstructured foil). The dashed line indicates the mean value of the data measured for the native *calamistrum*.

To mimic with a higher degree of exactness the *calamistrum's* hierarchical structures, i.e. micro-lines which are superimposed with nano-ripples (**Fig. 4A** and **B**), ultra-violet mask lithography was employed. Lines of 10 µm width, regularly distributed at 10 µm distance over an area of 3x3 cm² were fast and easily produced in SU-8 (Kayaku Advanced Materials, Inc.) (**Fig. 5A**). Further, the SU-8 lines were exposed to the KrF* laser beam, under different angles of incidence (3500 pulses at a fluence of 10-11 mJ/cm² and a repetition rate of 10 Hz). This resulted in nano-ripples with periods between 200 nm and 400 nm, and heights ranging between 60 nm and 100 nm. As this work is currently ongoing, peel-off measurements (as described in [8]) and adhesion measurements are in progress.

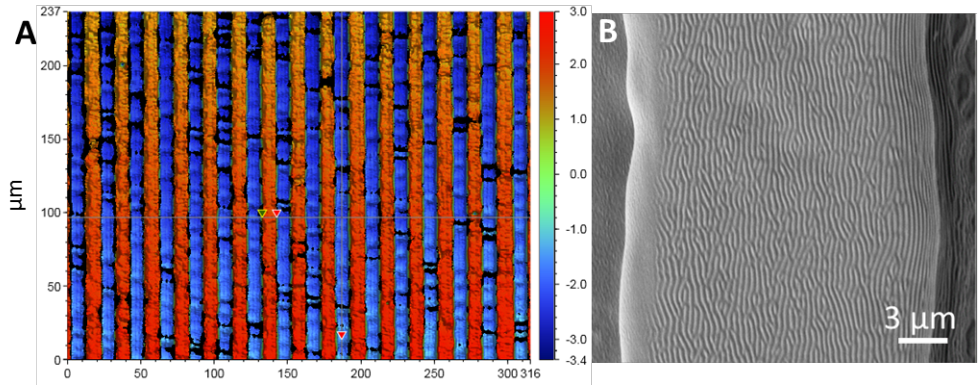

Fig. 4 (A) White light interferometry image of the lines produced in SU-8. (B) SEM of a SU-8 line which has been exposed to the KrF* laser at a 30° angle of incidence, showing nano-ripples with a spatial period of around 175 nm.

Considering that the nanofibers presented earlier are similar in diameter to the flagella and pili of bacteria, *Escherichia coli* (*E. coli*) TG1 bacteria were seeded onto PET samples (without ripples and with ripples of different spatial periods), to evaluate the effect of LIPSS on biofilm formation. To achieve nano-ripples of different spatial periods (ranging from approximately 200 nm to approximately 600 nm), the PET foils were exposed to the KrF* laser beam under six different angles of incidence (**Fig. 6A**) and with 6000 pulses at a repetition rate of 10 Hz using a fluence of 5.7-6.2 mJ/cm² [4]. When compared to non-irradiated surfaces (**Fig. 6B1**), laser-structuring of PET foils resulted in a significantly decreased cell adhesion (**Fig. 6B2-4)**. Spatial period plays a crucial role in bacterial adhesion – the smaller the spatial period is – the fewer cells attach to the nano-rippled

surface: the strongest reduction in cell adhesion (~91%) was observed for periods of 214 nm (**Fig. 5C)**.

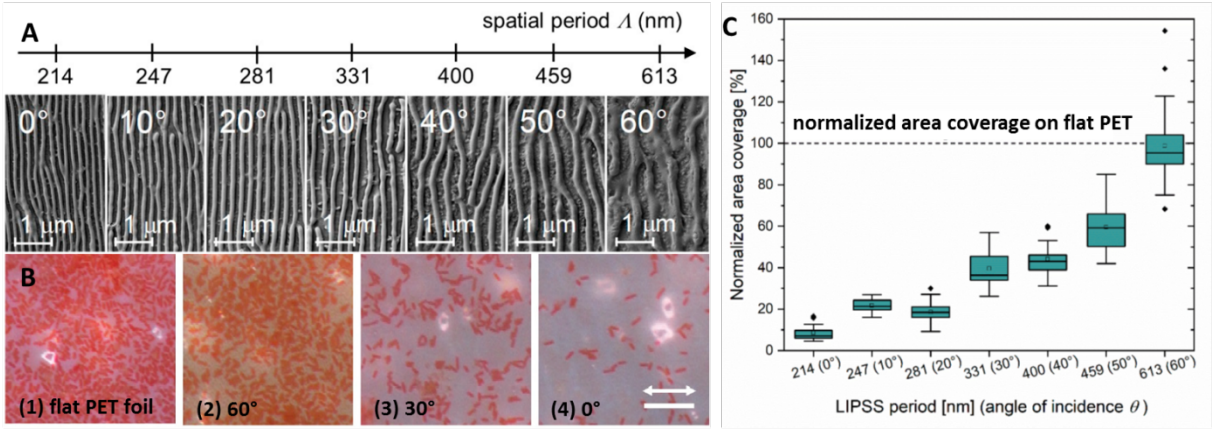

Fig. 5 (A) Nano-ripples with different spatial periods created by varying the laser beam incidence angle from 0° to 60°. (B) Optical reflected light microscopy of Safranine-stained *E. coli* TG1 on PET foils: (1) non-irradiated PET control sample; (2) laser-irradiated at θ = 60°; (3) 30° and (4) 0°. Scale bar 10 µm. Arrow indicates LIPSS orientation in images (2-4). (C) Surface area of laser-irradiated PET covered by *E. coli* TG1 cells normalized against non-irradiated control surface.

ACKNOWLEDGEMENTS:

This study has received funding from the European Union's Horizon2020 research and innovation programme under grant agreement No 862016 (BioCombs4Nanofibers, http://biocombs4nanofibers.eu).

REFERENCES

[1] C. Plamadeala, S.R. Gosain, F. Hischen, B. Buchroithner, S. Puthukodan, J. Jacak, A. Bocchino, D. Whelan, C. O'Mahony, W. Baumgartner and J. Heitz, "Bio-inspired microneedle design for efficient drug/vaccine coating", Biomed. Microdevices **22**, 8 (2020).

[2] A.-C. Joel, M. Meyer, J. Heitz, A. Heiss, D. Park, H. Adamova and W. Baumgartner, "A biomimetic comb as an antiadhesive tool to handle nanofibers", ACS Applied Nano Materials **3**, 3395-3401 (2020).

[3] R.-A. Barb, C. Hrelescu, L. Dong, J. Heitz, J. Siegel, P. Slepicka, V. Vosmanska, V. Svorcik, B. Magnus, R. Marksteiner, M. Schernthaner and K. Groschner, "Laser-induced periodic surface structures on polymers for formation of gold nanowires and activation of human cells", Appl. Phys. A **117**, 295-300 (2014).

[4] A.M. Richter, G. Buchberger, D. Stifter, J. Duchoslav, A. Hertwig, J. Bonse, J. Heitz and K. Schwibbert, "Spatial period of laser-induced surface nanoripples on PET determines *Escherichia coli* repellence", Nanomaterials **11**, 3000 (2021).

[5] F. Hischen, G. Buchberger, C. Plamadeala, O. Armbruster, E. Heiss, K. Winands, M. Schwarz, B. Jüttler, J. Heitz and W. Baumgartner, "The external scent efferent system of selected European true bugs (Heteroptera): a biomimetic inspiration for passive, unidirectional fluid transport", J. R. Soc. Interface **15,** 20170975 (2018).

[6] C. Plamadeala, S.R. Gosain, S. Purkhart, B. Buchegger, W. Baumgartner and J. Heitz, "Three-dimensional photonic structures fabricated by Two-Photon Polymerization for microfluidics and microneedles", ICTON 2018 Proceedings, 415-419 (2018).

[7] M. Meyer, G. Buchberger, J. Heitz, D. Baiko, A.-C. Joel, "Ambient climate influences anti-adhesion between biomimetic structured foil and nanofibers", Nanomaterials **11**, 3222 (2021).

[8] S. Lifka, K. Harsányi, E. Baumgartner, L. Pichler, D. Baiko, K. Wasmuth, J. Heitz, M. Meyer, A.-C. Joel, J. Bonse and W. Baumgartner, "Laser-processed antiadhesive bionic combs for handling of nanofibers inspired by nanostructures on the legs of cribellate spiders", Nanotechnology, *preprint*.

LIPSS FORMATION ON POLYMER THIN FILMS: INFLUENCE OF THICKNESS, ROUGHNESS AND SUBSTRATE

J. PRADA-RODRIGO[1,2], R.I. RODRÍGUEZ-BELTRÁN[1,3], J. CUI[4,5], A. NOGALES[4], T.A. EZQUERRA[4], P. MORENO[1], AND E. REBOLLAR[2*]

[1]Grupo de Aplicaciones del Láser y Fotónica (ALF-USAL), Universidad de Salamanca, Pl. de la Merced s/n, 37008, Salamanca, Spain
[2]Instituto de Química Física Rocasolano, IQFR-CSIC, Serrano 119, 28006, Madrid, Spain
[3]CONACYT- Centro de Investigación Científica y de Educación Superior de Ensenada, Unidad Foránea Monterrey, Alianza Centro 504, PIIT, Apodaca, Nuevo León CP 66629, México
[4]Instituto de Estructura de la Materia, Consejo Superior de Investigaciones Científicas (IEM-CSIC), Serrano 121, 28006 Madrid, Spain
[5]Key Laboratory of Surface & Interface Science of Henan Province, School of Material and Chemical Engineering, Zhengzhou University of Light Industry, Nº136, Science Avenue, Zhengzhou, Henan, 450002, China
*e.rebollar@csic.es

ABSTRACT

Laser induced periodic surface structures (LIPPS) have been formed on polymers using lasers with different wavelengths and pulse durations. Here, we focus on the influence of substrate nature and roughness, and film thickness on the formation of LIPSS using nanosecond and femtosecond laser pulses. In the case of nanosecond laser pulses at wavelengths efficiently absorbed by the polymer, we found that well-ordered LIPSS are formed for a range of thicknesses of polymer films supported on silicon substrates as well as on thicker free standing films. The results are explained considering the thermal properties of the materials. LIPSS can also be formed on polymer thin films despite the absence of light absorption at the wavelength of the irradiating laser by using a bilayer approach, employing as bottom layer another polymer which absorbs efficiently at the laser wavelength. In this case, for a thickness larger than a threshold value, no periodic structures are formed. This can be explained considering a mechanical restriction that prevents rearrangement of the bottom polymer film.

In the case of femtosecond pulses, for wavelengths in the UV region LIPSS are formed in both free standing and thin films deposited on different substrates while irradiation with near infrared femtosecond pulses lead to the generation of LIPSS only in the case of deposited thin films. Additionally, when the substrate is gold the influence of the gold substrate roughness and the polymer film thickness on LIPSS formation has been studied in terms of the features of the electric field distribution obtained by computer simulations. We obtain LIPSS as long as the aforementioned substrate and film parameters remain below certain threshold values. These experimental findings are explained by the formation and behavior of SPP in the thin film-substrate interface.

1. INTRODUCTION

It is widely accepted that LIPSS on the polymer surfaces originates from the interference between the incident and the surface scattered waves, which induced a heterogeneous intensity distribution, and together with a feedback mechanism results in the enhancement of the modulation intensity [1-2]. The features of LIPSS might be affected by the polymer properties, which are dependent not only on the chemical composition, but also on the polymer state, amorphous or semicrystalline, and on the hierarchical structure of the crystalline phase. It has been reported that when a polymer film is irradiated with a laser beam at a wavelength efficiently absorbed, the surface temperature increases. Thus, in order to obtain LIPSS, the temperature should be high enough to grant significant polymer chain mobility. In particular, temperature should be either above the glass transition temperature (Tg) for the case of amorphous polymer, allowing polymer chains to rearrange [3], or above its melting temperature (Tm) in the case of a semicrystalline polymer so that melting of the surface crystallites occurs providing enough polymer dynamics [4] and the redistribution of the material. In general, LIPSS can be prepared

in both spin-coated and in free standing polymer films, which makes LIPSS a potential method to obtain large processed surface area and good quality samples.

Film thickness may play also an important role on LIPSS formation. Csete et al. observed [5] that linear LIPSS are formed in films with thickness above a minimum thickness value. Also, substrate nature may affect LIPSS properties as reported by Kalachyova et al. [6] for doped poly(methyl methacrylate). P. Nürberger et al. [7] observed a change in orientation of LIPSS on a SiO2/Si layered system by varying the thickness of the dielectric SiO2 on the semiconducting Si substrate.

Here, we focus on the influence of the thickness of the polymer film in the form of thin films deposited over different substrates or as free-standing films, and of the substrates properties, on LIPSS formation. We use for that bot nanosecond laser pulses and femtosecond laser pulses.

2. LIPSS FORMATION USING NANOSECOND LASER PULSES

For inducing the formation of LIPSS on the surface of polymer films using nanosecond laser pulses it is important that the polymer absorbs at the laser irradiation wavelength. We have studied the influence of film thickness in the LIPSS formation using polystyrene (PS) films with thickness values ranging from 70 to 150×10^3 nm upon irradiation at 266 nm [8]. Films from 70 to 400 nm were casted on silicon and the thicker one is a free-standing film. The samples were irradiated at fixed values of fluence and number of pulses.

For the thinnest film, disordered LIPSS are formed. In contrast for thicker films, parallel ripples are observed. In the case of films with intermediate thicknesses, distorted LIPSS decorated with droplet-like entities can be observed. From the above results it is possible to conclude that, for silicon supported thin films, a critical range of film thicknesses exists at which the formation of well-ordered LIPSS is hindered. The laser irradiation of the PS films of different thicknesses provokes the substrate temperature to increase very fast. However, the heat is effectively dissipated on the basis of the high thermal diffusivity of silicon. Thus, the high thermal conductivity and thermal diffusivity of silicon makes the cooling of the polymer material heated by the laser pulse to be more efficient for thinner films. Accordingly, the silicon substrate acts as a thermal heat sink making that thinner films need more irradiation energy, either in terms of pulses of in term of fluence, in order to reach similar temperature values than those reached by thicker films.

In order to explain the singular behavior of the PS films with intermediate thicknesses values in the range 200–400 nm, for which droplet-like entities are observed, we can consider different facts. On the one hand, the heat dissipation by the substrate of the heat generated by surface irradiation is less efficient than for the thinnest film, but still it plays a role. On the other hand, we can consider the optical properties of the silicon, in particular the refractive index at 266 nm, which for silicon is higher than for PS. When the laser light reaches the silicon substrate the reflection from the substrate may introduce additional thermal effects and thus, less ordered LIPSS are expected.

In the case of polymers which do not absorb at the laser wavelength as is the case of the ferroelectric copolymer P(VDF-TrFE), which is transparent in all the UV-VIS-NIR range, LIPSS may be formed by using a bilayer approach. Nanostructuring of a bottom polymer layer, in this case P3HT, by laser irradiation, covered by a thin layer of P(VDF-TrFE), allows the development of a grating-like structure on the surface (Fig.1.a). The range of thicknesses of the upper layer which leads to the formation of LIPSS has been determined. In this case, for a thickness larger than 40 nm, no periodic structures are formed (Fig.1.b), neither in the upper layer nor in the bottom P3HT one. This can be explained considering a mechanical restriction which prevents P3HT rearrangement. P3HT cannot rearrange freely during the time it is melted and the formation of grating-like structure is not possible.

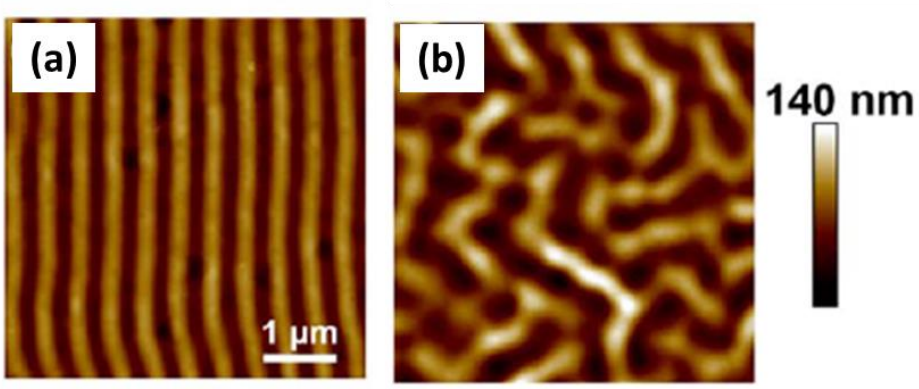

Fig.1. AFM topography images (5 μm×5 μm) of P3HT/P(VDF-TrFE) bilayer films irradiated with a fluence of 26 mJ/cm^2 and 3600 pulses: (a): P(VDF-TrFE) thickness: 20 nm (b) P(VDF-TrFE) thickness: 90 nm.

3.LIPSS FORMATION USING FEMTOSECOND LASER PULSES

We have experimentally observed that it was possible to induce the formation of LIPSS in polymer thin films by using both UV and NIR fs laser pulses. Irradiation of polymer thin films deposited on silicon, glass and gold and of thicker free-standing films with fs-UV pulses leads to the formation of LIPSS as a result of mechanisms analogous to those described for ns-UV pulses, because the materials studied have a high linear absorption coefficient in this region. It was also possible to nanostructure these polymers by irradiating them with fs-NIR pulses, where linear absorption is negligible. In this case LIPSS have been observed only on thin films deposited on the different substrates but they are not formed on the surface of free-standing films.

In a further step, polymer films of different thicknesses were deposited over gold substrates of different roughness and samples were irradiated with NIR fs pulses. We found LIPSS perpendicular to the laser polarization only for film thicknesses smaller than 150 nm deposited over the low roughness substrate. In order to evaluate how the substrate roughness and the thin film thickness affect the formation of surface plasmon polaritons (SPPs) and whether it can be related to the formation of LIPSS, we simulated the electromagnetic field resulting from the propagation and dispersion of the laser incident wave inside our samples and we compared the results to the experimental measurements. The results lead us to the hypothesis that the formation mechanism could be related to the SPP excited in the boundary between substrate and thin film. From our study of the penetration length we know that it must be similar to or smaller than the thickness of the thin film for SPP to intervene in LIPSS formation. In our experiments, we observe LIPSS for samples from 90 to 150 nm thick, which are in the range of SPP penetration distance. Consistently, we do not find LIPSS for thicker samples, as far as SPP cannot have any influence.

In our simulations, the intensity of the SPP increases with roughness (Rq) reaching a plateau above 20 nm. To sum up, the larger the Rq, the higher the coupling between the incident beam and the SPP, resulting in higher intensity. However, for Rq values higher than a certain threshold, periodicity is destroyed. Although there is a formation of hot spots on the surface, due to excessive scattering induced by oversized roughness, they cannot propagate to generate a periodic field. The final effect is a local field enhancement dependent on the specific roughness profile of the substrate but without periodicity. This explains why we do not observe LIPSS formation for the sample with the higher Rq substrate, but we do see an increase in its roughness after irradiation.

3.CONCLUSIONS

LIPSS can be obtained on the surface of polymer films deposited on silicon with different degrees of order by changing the polymer film thickness. The thinner and thicker films develop well ordered LIPSS, because in the first case the substrate acts as a thermal heat sink and in the second one surface heating effects are more relevant.

LIPSS can be prepared on polymer thin films, despite the absence of light absorption at the wavelength of the irradiating laser, by using a bilayer approach. But in this case, for a thickness of the upper layer larger than a certain threshold, no periodic structures are formed, neither in the upper layer nor in the bottom one. This can be explained by considering a mechanical restriction which prevents the rearrangement of the bottom layer.

LIPSS are formed on polymer films upon irradiation with fs pulses. UV fs pulses lead to the formation of LIPSS both on deposited films and free-standing film, while NIR fs pulses induce the formation of LIPSS only on deposited thin films. This indicates that different mechanisms take place at the different wavelengths. There is also an influence of the substrate. In particular, we have performed an experimental study and simulations of the influence of the substrate roughness and film thickness on the formation of LIPSS on polymer films deposited over gold with a near-infrared ultrashort pulsed laser. Experimentally we found LIPSS below threshold values of Rq and thin film thickness. However, above that threshold, we could not generate LIPSS. According to the simulations, for the gold substrate with high Rq, there is a large dispersion in the simulated period of SPP so that we cannot consider periodic structures, and for the thickest films, the penetration distance of the SPP is much smaller than the film thickness, so the coupling with the electric field at the film surface is negligible. We observe the same tendencies in the experimental period of LIPSS and the period of the SPP measured in the simulations. Both the experiments and simulations agree with the hypothesis that for LIPSS in thin films of a non-absorbing polymer deposited over a metal, the inhomogeneous electric field that starts the mechanism of LIPSS formation is the SPP generated in the thin film-substrate interface.

Acknowledgments
This work was funded by the Spanish State Research Agency (AEI) [project numbers PID2020-119003GB-I00/MCIN/AEI/10.13039/501100011033, PID2019-107514GB-I00/AEI/10.13039/501100011033, PID2019-106125GB-I00/AEI/10.13039/501100011033] and the Junta de Castilla y León [project number SA136P20]. J.P.-R. thanks the Spanish Ministry of Universities [grant number FPU17/01859].

REFERENCES

[1] E.Rebollar, D.Rueda, I. Martín-Fabiani, Á. Rodríguez-Rodríguez, M.C. García-Gutiérrez, G. Portale, M. Castillejo and T.A. Ezquerra, "In situ monitoring of laser-induced periodic surface structures formation on polymer films by grazing incidence small-angle X-ray scattering", Langmuir **31**, 3973-3981 (2015).
[2] M. Csete, S. Hild, A. Plettl, P. Ziemann, Z. Bor and O. Marti, "The role of original surface roughness in laser-induced periodic surface structure formation process on poly-carbonate films", Thin solid films **453-454**, 114-120 (2004).
[3] E. Rebollar, S. Pérez, J.J. Hernández, I. Martín-Fabiani, D.R. Rueda, T.A. Ezquerra and M. Castillejo, "Assessment and formation mechanism of laser-induced periodic surface structures on polymer spin-coated films in real and reciprocal space", Langmuir **27**, 55906-5606 (2011).
[4] Á. Rodríguez-Rodríguez, E. Rebollar, M. Soccio, T.A. Ezquerra, D.R. Rueda, J.V. Garcia-Ramos, M. Castillejo and M.-C. Garcia-Gutierrez, "Laser-induced periodic surface structures on conjugated polymers: poly (3-hexylthiophene)", Macromolecules **48**, 4024-4031 (2015).
[5] M. Csete, O. Marti and Z. Bor, "Laser-induced periodic surface structures on different poly-carbonate films", Appl. Phys. A **73**, 521-526 (2001).
[6] Y. Kalachyova, O. Lyutakov, P. Slepicka, R. Elashnikov and V. Svorcik, "Preparation of periodic surface structures on doped poly(methyl methacrylate) films by irradiation with KrF excimer laser", Nanoscale Res. Lett. **9**, 591 (2014).
[7] P. Nürnberger, H.M. Reinhardt, H.C. Kim, E. Pfeifer, M. Kroll, S. Müller, F. Yang, N.A. Hampp, "Orthogonally superimposed laser-induced periodic surface structures (LIPSS) upon nanosecond laser pulse irradiation of SiO 2 /Si layered systems", Appl. Surf. Sci. **425**, 682-688 (2017).
[8] J. Cui, A. Nogales, T.A. Ezquerra, E. Rebollar, "Influence of substrate and film thickness on polymer LIPSS formation", Appl. Sur. Sci. **394**, 125-131 (2017).

LIPSS WITH EXTREME PROPERTIES: SHORT PERIOD AND HIGH ASPECT RATIO

E. L. GUREVICH[1]*, A. DOSTOVALOV[2], AND A. KUCHMIZHAK[3]

[1] Laser Center (LFM), University of Applied Sciences Münster, Stegerwaldstraße 39, 48565 Steinfurt, Germany
[2]Institute of Automation and Electrometry of the SB RAS, 1 Acad. Koptyug Ave., 630090 Novosibirsk, Russia
[3] Institute of Automation and Control Processes, Far Eastern Branch, Russian Academy of Science, Vladivostok 690041, Russia
*gurevich@fh-muenster.de

ABSTRACT

In this talk parameters and mechanisms of the LIPSS formation with extreme characteristics (period and aspect ratio) on crystalline Si are discussed. We demonstrate transition from 250 nm to 70 nm period upon increasing the incident laser pulse number per site and explain our findings in the frames of the three-step LIPSS formation model, which combines electrodynamic and hydrodynamic processes. We also discuss why further decrease in the LIPSS period does not happen in silicon as the number of laser pulses is further increased. In the second part of the talk the LIPSS with high aspect ratio are demonstrated.

1. INTRODUCTION

The electrodynamic model describes appearance of the LIPSS as a result of interference between the incident laser light and the surface-scattered waves [1, 2]. It predicts that the period of the structure can be controlled primary by the wavelength of the incident laser light as well as by the refractive index of the sample and the environment [3]. The contrast of the interference pattern is not strong enough to cause any selective ablation only in the crests and no ablation in the troughs, hence hydrodynamic processes should be taken into account for correct description of the material redistribution in the melt [4]. The hydrodynamic processes can also induce periodic patterns in different systems lake e.g., phase transitions in solids, waves on liquid surfaces and melt solidification [5]. Here we demonstrate how the combination of the electrodynamic and hadrodynamic models [6] helps explaining the LIPSS periods observed in experiments.

2. LIPSS WITH PERIOD $\Lambda \approx 70\,$nm

LIPSS were formed on a crystalline Si surface exposed to multiple $\tau_p \approx 180\,$fs laser pulses, central wavelength $\lambda = 515\,$nm, The pulse fluence $F = 0.09\,J/cm^2$ was below the single-pulse ablation threshold. The silicon sample was immersed in different liquids during the laser processing, see [7] for more experimental details. The experiments demonstrate that as the scanning velocity decreases (i.e., the pulse overlap or the number of pulses per site increases) the period of the LIPSS jumps from $\Lambda_1 \approx 250 \pm 20\,$nm to $\Lambda_2 \approx 70 \pm 10\,$nm. Interestingly, the same period change was observed in experiments with silicon immersed in liquid precursors for metallic nanoparticles, where the nanoparticles were generated together with the LIPSS [8]. This observation proves that the refractive index of the Si-liquid interface cannot explain the period change observed in the experiments.

Our results can be explained if we treat the LIPSS formation as a sequence of two events: (1) incident light scattering on the surface roughness [1]; (2) development of the ablative Rayleigh-Taylor instability in the melt [4]. The decrease in the period of the structures happens *after* the first LIPSS with $\Lambda_1 \approx 250\,$nm is formed on the surface. At low scanning speed the incident light continues illuminating the surface, on which the large-period LIPSS are formed. Now the following incident laser pulses are scattered by a regular periodic pattern with $\Lambda_1 \approx 250\,$nm, but not by the random surface roughness as it was in the beginning.

The period of the interference pattern formed by overlapping the incident and the scattered waves in this case will be shifted to $\Lambda_2 \approx 70\,\text{nm}$ [9, 7]. The sequence of these events is schematically shown in Fig. 1, in which the laser beam scans the surface from left to right.

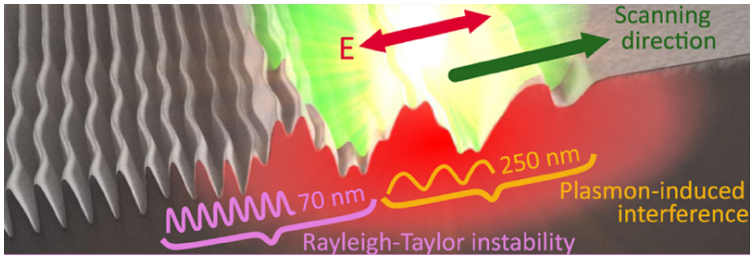

Fig. 1: Formation of LIPSS with $\Lambda \approx 70\,\text{nm}$. Modified from [7].

A further reduction in the scanning speed or multiple surface scanning with the same laser parameters should result in the next LIPSS period reduction: The incident laser pulses should be scattered by the periodic structure with $\Lambda_2 \approx 70\,\text{nm}$ and form LIPSS with $\Lambda_3 \approx 40\,\text{nm}$ [9]. However this does not happen. This predicted period reduction does not occur, since the relocation of the melt on the surface is driven by the Rayleigh-Taylor instability, which fastest growing mode for the given experimental conditions is at $\Lambda \approx 80 - 100\,\text{nm}$, i.e., very close to the observed small LIPSS period of 70 nm. The expected (but not observed) next LIPSS period of $\Lambda_3 \approx 40\,\text{nm}$ is smaller than the critical period of the instability, hence, it cannot grow.

3. LIPSS WITH HIGH ASPECT RATIO

In the second part of the talk, we describe experiments [10], in which the Si surface was first coated with a thin Hf layer of 20 nm, which melting point ($T^m_{Hf} \approx 2500\,\text{K}$) and the boiling point ($T^b_{Hf} \approx 5400\,\text{K}$) are much higher than that of Si ($T^m_{Si} = 1683\,\text{K}$ and $T^b_{Si} = 3533\,\text{K}$). Femtosecond laser pulses at $\lambda = 1026\,\text{nm}$ were used to make LIPSS in ambient environment and under nitrogen atmosphere. The cross section of such LIPSS structure is shown in the scanning electron microscope image in Fig. 2. Remarkably, the depth-to-width ratio of these LIPSS is up to approximately 8:1.

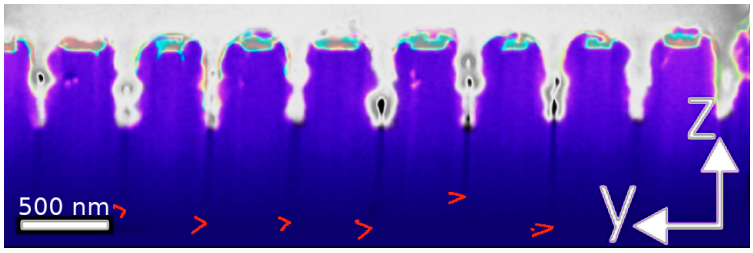

Fig. 2: LIPSS in Si covered with Hf with high aspect ratio. The bottoms of the periodic cracks are marked with red arrows in the picture, while the epoxy glue could not completely penetrate such deep groves. Modified from [10].

The physical processes leading to such a high depth-to-width aspect ratio are not completely clear. Probably, during the laser processing the Si substrate melts below the solid Hf layer at the initial stage of the process. The interference between the incident and the surface waves modulates the surface temperature (of both Hf and Si) periodically, silicon melts, but the material redistribution is suppressed by the solid layer of Hf on the top. Presumably, the temperature and the amplitude of the temperature modulation in Si grows further and may reach the boiling point T^b_{Si} until the Hf overlayer melts and breaks, releasing the overheated Si. After the surface Hf layer breaks, the sample surface looks like a regular set of narrow trenches. The high-aspect ratio LIPSS appear only when the polarisation of the incident light is oriented perpendicular to the orientation of these trenches, suggesting that the incident electromagnetic wave is amplified by the periodic Hf structure.

REFERENCES

[1] D. C. Emmony, R. P. Howson and L. J. Willis, "Laser mirror damage in germanium at 10.6 μm." Appl. Phys. Lett., **23**, 598 (1973).

[2] J. Sipe, J. F. Young, J. Preston, and H. Van Driel, "Laser-induced periodic surface structure. I. Theory." Phys. Rev. B **27**, 1141 (1983).

[3] T. J.-Y. Derrien, J. Krüger, J. Bonse, "Properties of Surface Plasmon Polaritons on Lossy Materials: Lifetimes, Periods and Excitation Conditions." J. Opt. **18**, 115007 (2016).

[4] E. L. Gurevich, "Mechanisms of femtosecond LIPSS formation induced by periodic surface temperature modulation." Applied Surface Science **374**, 56 (2016).

[5] M. C. Cross and P. C. Hohenberg, "Pattern formation outside of equilibrium." Reviews of Modern Physics, **65**, 851 (1993).

[6] E. L. Gurevich, Y. Levy, N. M. Bulgakova, "Three-step description of single-pulse formation of laser-induced periodic surface structures on metals." Nanomaterials **10**, 1836 (2020).

[7] Yu. Borodaenko, S. Syubaev, S. Gurbatov, A. Zhizhchenko, A. Porfirev, S. Khonina, E. Mitsai, A. V. Gerasimenko, A. Shevlyagin, E. Modin, S. Juodkazis, E. L. Gurevich, A. A. Kuchmizhak, "Deep Subwavelength Laser-Induced Periodic Surface Structures on Silicon as a Novel Multifunctional Biosensing Platform." ACS Applied Materials & Interfaces, **13**, 54551-54560 (2021).

[8] Yu. Borodaenko, S. Syubaev, E Khairullina, I. Tumkin, S. Gurbatov, A. Mironenko, E. Mitsai, A. Zhizhchenko, E. Modin, E. L. Gurevich, A. A. Kuchmizhak, "On-Demand Plasmon Nanoparticle-Embedded Laser-Induced Periodic Surface Structures (LIPSSs) on Silicon for Optical Nanosensing." Adv. Optical Mater., 2201094 (2022).

[9] E. L. Gurevich, S. V. Gurevich, "Laser induced periodic surface structures induced by surface plasmons coupled via roughness." Applied Surface Science **302**, 118 (2014).

[10] K. Bronnikov, A. Dostovalov, V. Terentyev, S. Babin, A. Kozlov, E. Pustovalov, E. L. Gurevich, A. Zhizhchenko, A. Kuchmizhak, "Uniform subwavelength high-aspect ratio nanogratings on metal-protected bulk silicon produced by laser-induced periodic surface structuring." Appl. Phys. Lett. **119**, 211106 (2021).

SURFACE MORPHOLOGY AT NANOMETRIC SCALE BY TEMPORAL AND POLARIZATION CONTROL OF ULTRASHORT LASER PULSES

A. NAKHOUL[1,2], C. MAURICE[2], F. GARRELIE[1], F. PIGEON[1], J-P. COLOMBIER[1]

1- Univ Lyon, UJM-Saint-Etienne, CNRS, IOGS, Laboratoire Hubert Curien UMR5516, F-42023 St-Etienne, France3- Address of author3 if different

2- Mines Saint-Etienne, Univ. Lyon, CNRS, UMR 5307 LGF, Centre SMS, F - 42023 Saint-Etienne, France

Abstract.

Ultrafast-laser irradiated surface is a typical paragon of a self-organizing system, which emerge and organize complex micropatterns and even nanopatterns. A spectacular manifestation of dissipative structures consists of different types of randomly and periodically distributed nanostructures that arise from a homogeneous metal surface. The formation of nanopeaks, nanobumps, nanohumps and nanocavities patterns with 20–80 nm transverse size unit and up to 100 nm height are reported under femtosecond laser irradiation with a regulated energy dose [1, 2]. We shed the light on the originality of the nanopeaks, having an exceptional aspect ratio on the nanoscale [3]. They are primarily generated on the crests grown between the convective cells formed by the very first pulses. The production of these distinct nanostructures can enable unique surface functionalizations toward the control of mechanical, biomedical, optical, or chemical surface properties on a nanometric scale [4-7]. We show that the use of crossed-polarized double laser pulse adds an extra dimension to the nanostructuring process as laser energy dose and multi-pulse feedback tune the energy gradient distribution, crossing critical values for surface self-organization regimes. Furthermore, the initial surface roughness and type of roughness is another essential feature to be controlled to switch from a regime of self-organization to another one.

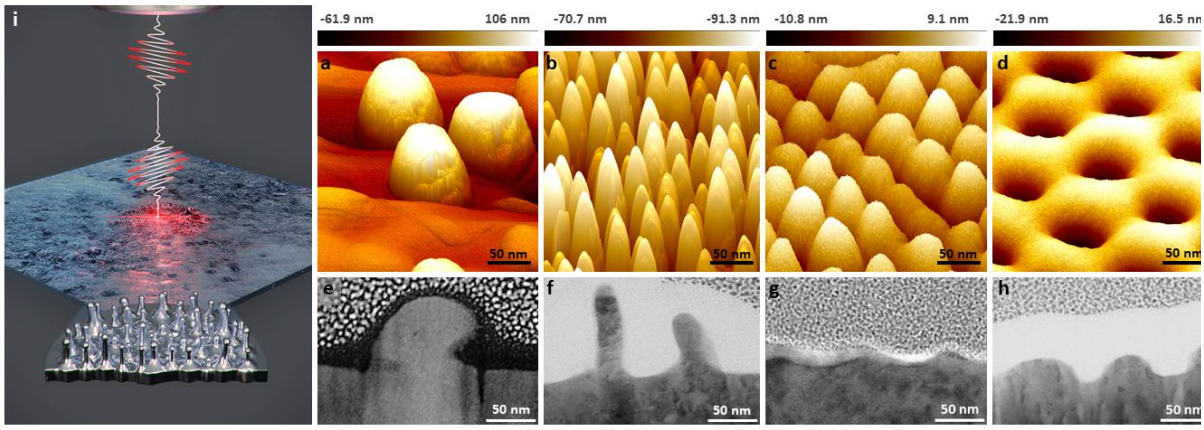

Figure 1. 3D atomic force microscopy of the nanobumps (a), nanopeaks (b), nanohumps (c) and nanocavities (d) presenting the nanostructures height and distribution. (e-h) Transmission electron microscopy of the principles nanstructures presenting the cross view of nanostructures. (i) Schematic illustration of nanopeaks formation by femtosecond laser double pulse.

[1] A. Nakhoul, C. Maurice, M. Agoyan, A. Rudenko, F. Garrelie, F. Pigeon, J.-P. Colombier, "Self-Organization Regimes Induced by Ultrafast Laser on Surfaces in the Tens of Nanometer Scales", Nanomaterials **11** (2021).
[2] A. Abou Saleh, A. Rudenko, S. Reynaud, F. Pigeon, F. Garrelie, J.-P. Colombier, "Sub-100 Nm 2D Nanopatterning on a Large Scale by Ultrafast Laser Energy Regulation", Nanoscale **12** 6609–6616 (2020).
[3] A. Nakhoul, A. Rudenko, C. Maurice, S. Reynaud, F. Garrelie, F. Pigeon, J.-P. Colombier, "Boosted Spontaneous Formation of High-Aspect Ratio Nanopeaks on Ultrafast Laser-Irradiated Ni Surface", Adv. Sci. **21** 2200761 (2022).
[4] Z. Wu, K. Yin, J. Wu, Z. Zhu, J.-A. Duan, J. He, "Recent Advances in Femtosecond Laser-Structured Janus Membranes with Asymmetric Surface Wettability", Nanoscale **13** 2209–2226 (2021).
[5] V. Zorba, E. Stratakis, M. Barberoglou, E. Spanakis, P. Tzanetakis, S.H. Anastasiadis, C. Fotakis, "Biomimetic Artificial Surfaces Quantitatively Reproduce the Water Repellency of a Lotus Leaf", Adv. Mater. **20** 4049–4054 (2008).
[6] A. Elbourne, R.J. Crawford, E.P. Ivanova E.P, "Nano-structured antimicrobial surfaces: From nature to synthetic analogues J. Colloid Interface" Sci. **508** 603–616 (2017).
[7] J. Bonse, R. Koter, M. Hartelt, D. Spaltmann, S. Pentzien, S. Höhm, A. Rosenfeld, J. Krüger, "Tribological Performance of Femtosecond Laser-Induced Periodic Surface Structures on Titanium and a High Toughness Bearing Steel", Appl. Surf. Sci. **336** 21–27 (2015).

STOCHASTICITY VERSUS DETERMINISM IN LIPSS FORMATION

J.P. COLOMBIER[1]*, E. BRANDAO[1], A. NAKHOUL[1], R. EMONET[1], F. GARRELIE[1], A. HABRARD[1], F. JACQUENET[1], F. PIGEON[1], A. RUDENKO[1], M. SEBBAN[1]

[1] Univ Lyon, UJM-Saint-Etienne, CNRS, IOGS, Laboratoire Hubert Curien UMR5516, F-42023 St-Etienne, France
*jean.philippe.colombier@univ-st-etienne.fr

ABSTRACT

Understanding the spontaneous emergence of patterns on laser-irradiated surface has been a topic of interest for many years. Brought far from equilibrium under ultrafast photoexcitation, the material exhibits topographic surfaces that reveal signatures from multiphysical coupling, interrogating on the principal mechanism that drives the organisation nature. Some laser-induced periodic surface structures reveal periods typic from electromagnetics, nonlinear optics and plasmonic origin whilst others are characteristic of fluid dynamics or even thermochemical reactions. However, upon multi-shot irradiation, liquid flows are driven by laser-induced energy gradients and patterns are unstable leading to a variety of possible states, including hybrid states of bistable patterns and chaos. Stable spatially-periodic patterns typically arise through small, localized perturbations of the underlying optical coupling on random nanoreliefs. These perturbations grow in amplitude until nonlinear saturation takes over while, at the same time, the nascent topography disturbs the optical response. Whereas the spatially uniform growth into a pattern that can be described within the classic Maxwell and Navier-Stokes equations, the propagation, spatial competition of modes and bifurcation regime require nonlinear dynamics that mimic the behavior of the excited systems near the onset of convective instabilities. One of the challenges is to develop a general and efficient model that inherit relevant symmetry and scale invariance properties and that contain the stochasticity (emergence) and nonlinear properties (dynamics) able to reproduce dissipative structures in spatially extended systems. A stochastic Swift-Hohenberg modelling is then proposed to reproduce hydrodynamic fluctuations at the convective instability threshold that has been recently demonstrated as the very nature of the laser-induced self-organized nanopatterns.

1. DETERMISTIC APPROACH

The issue of laser-induced self-organization of the surface at the nanoscale, originating in near-field light-matter coupling, carries strong scientific weight as it puts forward the question on localizing light on extreme scales [1-2]. Along with the experimental achievements, we have developed a model combining three-dimensional electromagnetic and hydrodynamic approaches to deliver a comprehensive frame for understanding light-induced structuring on tens of nanometer scales [3]. The numerical calculations allow us to investigate the multipulse evolution of surface relief in a self-consistent way, evaluating both the inhomogeneous absorption due to surface roughness and the thermomechanical flows. Activated by transverse temperature gradients resulting from complex light coupling on the surface, we observed that the melt flow follows Marangoni surface tension forces. Destabilized by the associated rarefaction wave, we showed that a convection instability develops in thin laser-melted layers up to surface resolidification. This hydrodynamic instability, analog to the Bénard-Marangoni one, drives the matter towards self-organized convection nanocells and, being sensitive to polarization dependence, can induce thermocapillary waves by transverse surface tension gradients. These result in periodic stripes with subwavelength spacings, corresponding to high-spatial frequency LIPSS formation and also to hexagonal convection cell patterns if the polarization dependence is intentionally erased. Coupling electromagnetism to hydrodynamics enables to numerically replicate the different types of periodic structures commonly observed on metal surfaces, their precursors, origins of their periodicity and orientation, and plausible feedback mechanisms for their formation up to the formation of nanopeaks [4].

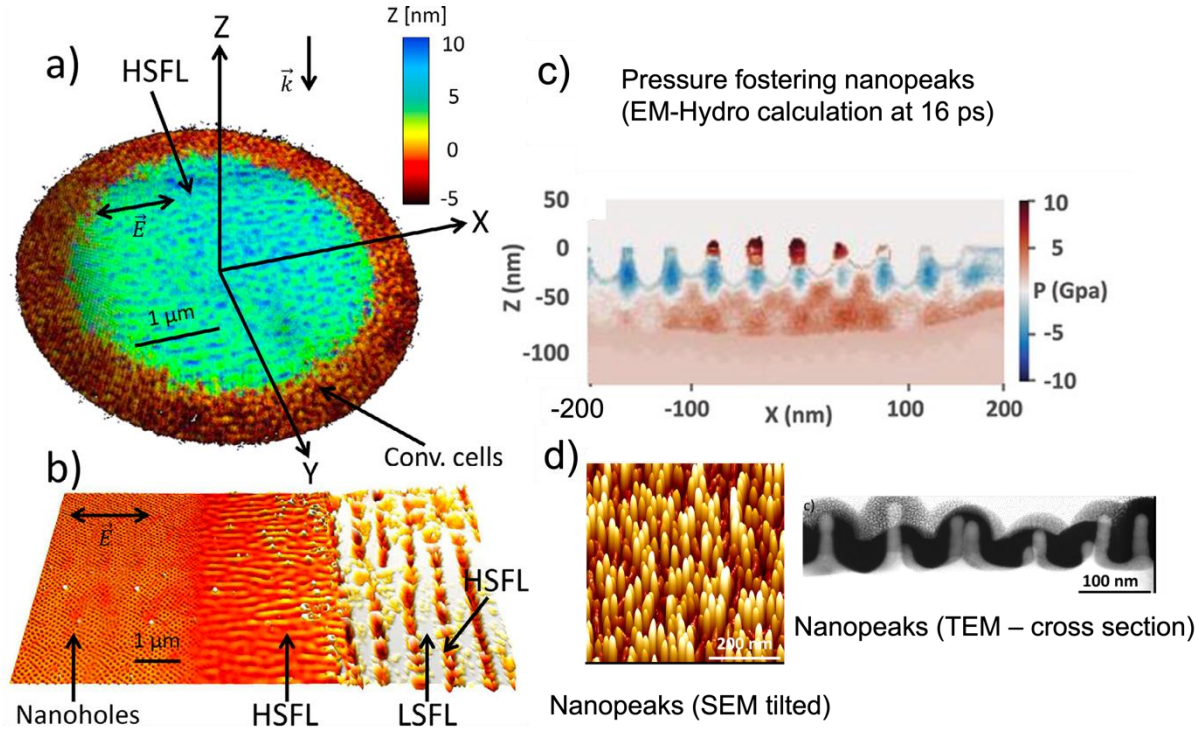

Fig. 1 Comparison between EM-hydrodynamics simulations (a-c) with experimental SEM images (b-d) for nanocavity and HSFL formation conditions (a-b) and nanopeaks generation (c-d) upon ultrafast laser irradiation (100 fs duration). A double-pulse irradiation sequence (25 pulses) with crossed linear polarization has been used to generate the structures. The delay between sub-pulse and the local fluence regulate the kind of patterns.

The results presented in Fig.1 deliver a comprehensive frame for the understanding of light-induced structuring on record scales as we elucidate that the generation of HSFL, hexagonal lattice and nanopeaks formation result from the interplay between non-radiative optical response on surface and surface-tension driven flows, leading to the development of Marangoni convection instability [4]. The optical and then thermoconvective response of a set of asperities now offers a unique process for manufacturing self-organized structures, porous or super-rough surfaces with a resolution of about ten nanometers.

2. NONLINEAR DYNAMICS APPROACH

From a formal point of view, the obtained pattern resulting from convective instability, is initiated by energetical fluctuation effects due to near fields on the surface. Technically, a noise term has been added to the surface topography fostering a strong inhomogeneous absorption that disturbs in turn the uniform response of the deterministic equations of hydrodynamics. Noise-driven unexpected symmetry of patterns and chaos offer a self-consistent framework towards realistic situations in laser-surface situations. However, to advance the understanding of complex dynamics in the presence of fluctuations at the onset of fluid instability, a nonlinear mathematical approach enabling to predict Turing-like patterns resulting to self-organization is proposed.

In convective systems literature, many works investigate self-organized features based on the Swift-Hohenberg model, especially related to the stability of stationary solution and pattern selections as well as the in influence of stochastic external noise. For dissipative dynamical systems, the existence of global attractors, namely a fully invariant and attracting pattern, has been proved.

For Rayleigh-Bénard convection, the Swift-Hohenberg model follows from a 2D projection of the governing fluid equations in the Boussinesq approximation that eliminates the dependence of the temperature, pressure, and velocity fields on the coordinate normal to the surface during the hydrodynamic instabilities.

The SH equation has been intensely investigated as a simplified model to understand the key pattern forming mechanisms and to provide insight into the dynamics of pattern formation in complicated systems. The variety of pattern-like solutions of the SH equation still constitutes an active research topic. Laser-induced pattern formation at the nanoscale can be efficiently characterized and predicted by this kind of stochastic model which is variational in time and conservative in space. Varying the model coefficients (namely a nonlinear strength and a bifurcation parameter that measures the dimensionless distance to the convection threshold in terms of the Rayleigh number) allow to reliably reproduce the nanostructures. Pattern-like solutions of the SH equation are remarkably similar to the ones that we can observe in the irradiated surfaces Scanning Electron Microscope (SEM) images, as can be seen in Fig. 2.

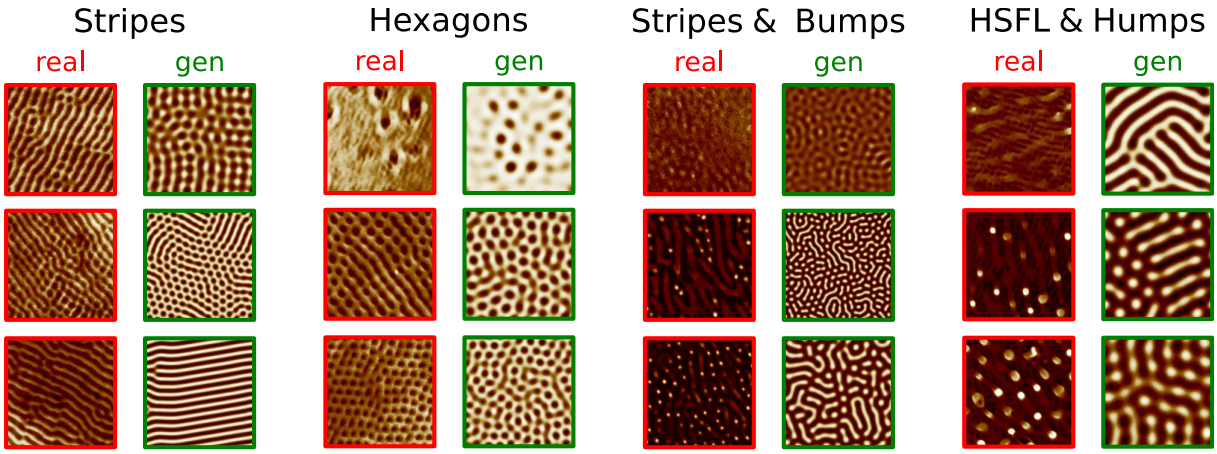

Fig. 2 Comparison between real SEM images (red) and SH-generated images (green). SH generated images are able to reproduce a variety of patterns (e.g., stripes, hexagons, bumps, HSFL, humps) and scales [5]. Since the SH model is an isotropic model, global symmetries are only apparent (e.g., oriented stripes), whereas SEM images retain some measure of global symmetry from laser polarization.

We reveal that the complexity of surface 2D patterns emergence can be learned by a deep convolutional network to connect the model coefficients to the experimental irradiation parameters, providing key process parameters to design a specific pattern [5]. Scale invariant, the model has been finally calibrated on experimental microscopy measurements evidencing that relevant timescale of convective instability process can be derived by this system dynamics modelling.

REFERENCES

[1] R. Stoian and J.P. Colombier, “Advances in ultrafast laser structuring of materials at the nanoscale”, Nanophotonics 9(16), 4665-4688 (2020).

[2] A. Abou Saleh, A. Rudenko, S. Reynaud, F. Pigeon, F. Garrelie, & J.P. Colombier, “Sub-100 nm 2D nanopatterning on large scale by ultrafast laser energy regulation”, Nanoscale **12** (12), 6609 (2020).

[3] A. Rudenko, A. Abou-Saleh, F. Pigeon, C. Mauclair, F. Garrelie, R. Stoian, & J. P. Colombier “High-frequency periodic patterns driven by non-radiative fields coupled with Marangoni convection instabilities on laser-excited surfaces” Acta Materiala **194**, 93 (2020).

[4] A. Nakhoul, A. Rudenko, C. Maurice, S. Reynaud, F. Garrelie, F. Pigeon, and J.P. Colombier, “Boosted Spontaneous Formation of High-Aspect Ratio Nanopeaks on Ultrafast Laser-Irradiated Ni Surface”, Advanced Science, **9** (21) 2200761 (2022).

[5] E. Brandao, J.P. Colombier, S. Duffner, R. Emonet, F. Garrelie, A. Habrard, F. Jacquenet, A. Nakhoul and M. Sebban. “Learning PDE to Model Self-Organization of Matter”, Entropy, **24** (8), 1096 (2022).

INVESTIGATION OF LIPSS STRUCTURES FABRICATED IN DIFFERENT SURROUNDING MEDIA USING FOCUSED-ION BEAM ETCHING

M. SENEGAČNIK, P. GREGORČIČ

Faculty of Mechanical Engineering, University of Ljubljana, Aškerčeva 6, 1000 Ljubljana, Slovenia

matej.senegacnik@fs.uni-lj.si

In this study, we investigate the influence of different media surrounding the laser irradiation spot on the characteristics of the formed laser-induced periodic surface structures (LIPSS). The surrounding media used in the experiments include air, nitrogen, and argon, which mainly affect the chemical composition of the treated surface, while water and polyethylene glycol 300 are used to study the effects of cavitation bubbles that occur in liquids during laser processing. Stainless steel and titanium samples are irradiated with 45 ns and 30 ps polarized laser pulses, emitted by a nanosecond fiber laser (λ = 1060 nm) and a Nd:YAG picosecond laser (λ = 1064 nm), respectively. Variation of the surrounding media [1] and laser processing parameters [2], including pulse fluence, beam scanning velocity, and pulse duration, results in different characteristics of the structures [3] formed in the upper layer of the irradiated material.

In gas atmospheres, when longer nanosecond pulses are used for LIPSS generation, we observe mainly the effect of surface oxidation, while the topographic change (typical for LIPSS at shorter pulses) is almost negligible (Fig. 1a). Interestingly, the oxide layer thickness changes periodically, with a period typical for LIPSS formation. Thus, in this case, LIPSS composes of a thin periodic oxide layer with a thickness of several tens of nanometers. Slight variations in pulse fluence and beam scanning velocity appear to change the characteristics of the oxide layer, which we investigate by cross-cutting (Fig. 1a) and etching (Fig. 1b) the samples with a focused ion beam (FIB). The chemical composition of the upper surface layer is analyzed by energy-dispersive X-ray spectroscopy (EDS) and X-ray photoelectron spectroscopy (XPS).

In liquid environments, we observe the formation of LSFL and HSLF at high pulse overlap, where the liquid viscosity and beam scanning velocity affect the spatial period and repeatability of the fabricated structures. At low pulse overlap, laser-induced cavitation bubbles play a more important role and can lead to formation of curved microgrooves under suitable conditions (Fig. 1c). We assume that the microgrooves in this regime are formed by the modulation of the laser beam intensity at the interface of the generated cavitation bubbles, which act as diffraction objects [4]. When the beam is scanned in altering directions within this regime, meandering structures with ~20 μm radius of curvature are created.

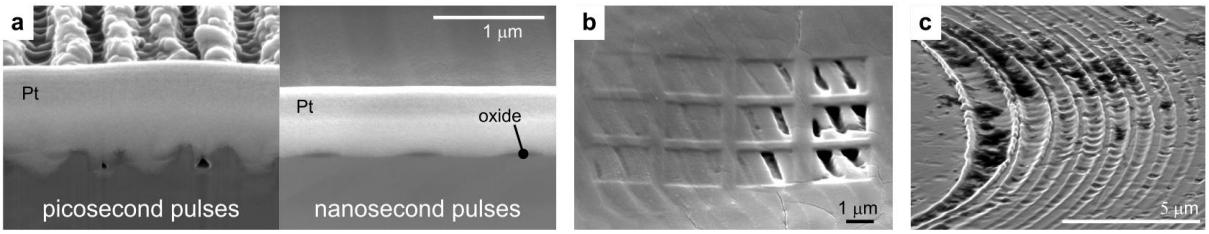

Figure 1. (a) Cross-sections of LIPSS obtained in air atmosphere by picosecond and nanosecond pulse irradiation. (b) Etching the top surface of LIPSS with a FIB. (c) Curved microgrooves obtained by laser irradiation in liquid.

[1] S. Maragkaki, A. Elkalash, E.L. Gurevich, Orientation of ripples induced by ultrafast laser pulses on copper in different liquids, Applied Physics A, **123**, 721, (2017).

[2] M. Senegačnik, M. Hočevar, P. Gregorčič, "Influence of processing parameters on characteristics of laser-induced periodic surface structures on steel and titanium", Procedia CIRP, **81**, 99, (2019).

[3] J. Bonse, J. Krüger., S. Höhm, A. Rosenfeld, Femtosecond laser-induced periodic surface structures, Journal of Laser Applications, **24**, 042006, (2012).

[4] M. Senegačnik, P. Gregorčič, submitted for publication, (2022).

MICROSCOPY TECHNIQUES FOR IN-SITU LIPSS DETECTION AND CHARACTERIZATION VIA OPTICAL MEANS

C. MAUCLAIR[1], A. AGUILAR[1], X. SEDAO[1], JEAN-PHILIPPE COLOMBIER[1], RAZVAN STOIAN[1]

[1]Laboratoire Hubert Curien, UMR 5516 CNRS, Université de Lyon, Université Jean Monnet, 42000, St. Etienne, France

*cyril.mauclair@univ-st-etienne.fr

ABSTRACT

Surpassing the diffraction limit on optical microscopy has lead to important breakthroughs in recent years, especially in the biomedical field, where it is common practice to add a functional group to the biological samples such as fluorophores. However, in applications involving surface micro-nano-structuration and particularly when Laser Induced Periodic Surface Structures are achieved by ultrafast laser irradiation, there is an interest in analyzing these non fluorescent surfaces using non-contact optical techniques. In this report, a wide field super resolution technique, the structured illumination microscopy (SIM), is adapted to observe metallic surfaces. We verify that the technique permits to surpass the diffraction limit by a factor of two. Laser-induced surface micro-structures on stainless steel are characterized with the expected super resolution. The technique enables in-situ characterization of the LIPSS pattern and permits to follow its formation during a multipulse irradiation sequence. We also discuss the potential of another optical technique, namely the Fourier Ptychography Microscopy that permits to overcome the resolution limit of the observing lens by high angle illumination while preserving the large field of view with proof of concept results on a sector resolution target.

1. INTRODUCTION

The generation of Laser Induced Periodic Surface Structures (LIPSS) has attracted a worldwide attention due to the possibility to obtain micro and submicrometric structuring on various substrates with the flexibility of the laser irradiation tool. Many application fields are impacted by LIPSS, mostly related to adding functions to surfaces like hydrophobicity, optical properties and cellular differentiation [1-3]. When using ultrafast laser pulses for surface structuring, the low onset of thermal effects at low repetition rate enlarges the laser process parameters to observe LIPSS formation. Moreover, various kinds of LIPSS are made distinguishable by finely tuning the irradiation conditions of the ultrafast pulses in terms of pulse energy, repetition rate, polarization and so on.

Fine characterization of LIPSS is usually conducted by ex-situ analysis using atomic force microscopy

(AFM) and scanning electron microscopy (SEM). However, these types of post mortem measurements do not allow to easily observe the pulse to pulse evolution of the LIPSS pattern directly within the irradiation set-up. In the following, we discuss the interest of two optical techniques, namely structured illumination microscopy (SIM) and Fourier Ptychograph Microscopy (FPM) for in-situ analysis of micrometric and submicrometric surface structures.

2. SIM FOR IN-SITU LIPSS CHARACTERIZATION

We have recently proposed the use of SIM to characterize the LIPSS formation [4]. By projecting a series of periodic illuminations with a period equal to the objective diffraction limit, a super resolution image with spatial frequencies two times higher than the objectif cutoff frequency can be recontructed [5] (see Fig. 1). In our case, using an UV LED at $\lambda = 405$ nm with an objective of NA = 0.9, yields a Rayleigh criterion of $k_o = 275$ nm. Experimentally, the SIM set-up was to shown to reach a lateral resolution of 155 nm, which is close enough to the theoretical goal of 138nm and sufficient to clearly observe ultrafat-laser induced Low Spatial Frequency LIPSS (LSFL) on metallic glass whose period lies within the 600-700nm range.

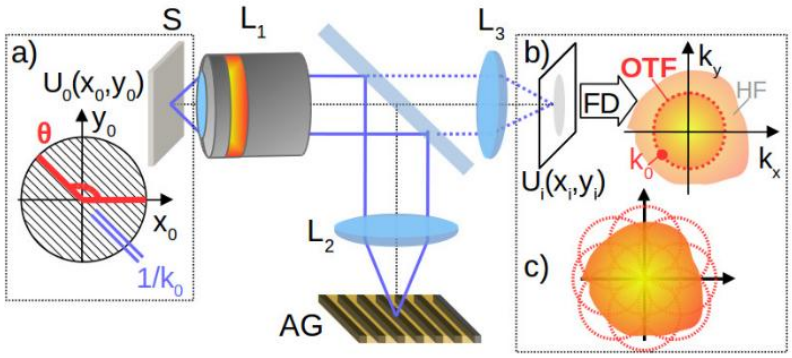

Fig. 1 SIM adapted to LIPSS imaging in reflexion. a) An amplitude grating (AG) is projected on the sample (S) by the 4f system (objective L1 +lens L2). The microscope image field is formed by L3 on the CCD. b) Microscope OTF in the frequency domain (FD) with illustration of the super resolution reconstruction c) for the sample high frequencies (HF).

Figure 2 depicts a comparison of SIM with SEM and regular brightfield optical microscopy (OM). There, it is clear that SIM enables an optical characterization in situ with a sufficient imaging resolution to clearly follow the LIPSS pattern evolution during the multipulse irradiation sequence.

As discussed more in details in [4], several physical mechanisms leading to the formation of the LSFL could be unveiled using the technique such as a phase-locking mechanism that stabilizes and amplifies the ordered corrugation during the multipulse irradiation sequence (not shown here).

If the technique allows for submicrometric in-situ and non-contact analysis of LIPSS, there is not doubt about its interest for ultrafast laser surface structuring applications where this analysis can obviously be utilized as a real-time feedback for process control. However, the sample surface field that can be imaged with SIM is restricted to the objective lens field of view which is typically of a few tens of µm for high NA objectives. This can be a limitation when larger characterization areas are required. Moreover, the working distance of this type of objective is usually very short, below 1 mm. These issues can both be adressed with the technique of Fourier Ptychography Microscopy which is discussed hereafter.

3. FPM FOR IN-SITU LARGE FIELD SURFACE ANALYSIS

Recently, the development of FPM (Fourier Ptychography Microscopy) has drawn a remarkable attention in the field of biomedical imaging [6]. FPM offers the possibility to reconstruct a high resolution image from a series of low resolution acquired through a low NA objective lens with high angle illumination.

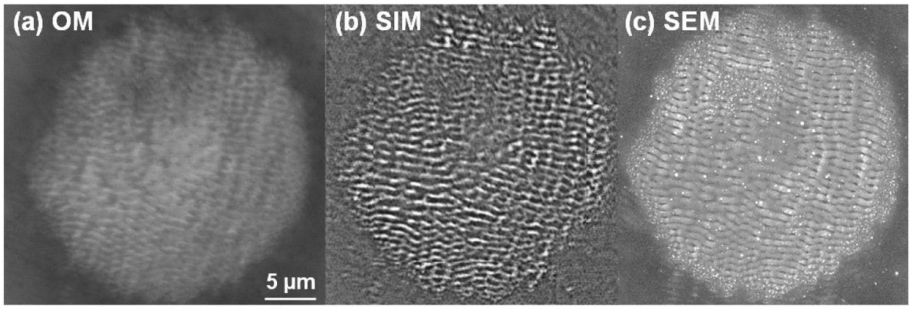

Fig. 2 Visualization of sub-wavelength LIPSS on a metallic glass (Zr-based) surface created after 5 ultrafast laser pulses using a peak fluence of 0.3 J/cm 2 . The same pattern is visualized by a range of imaging techniques. (a) Impact zone observed using a conventional bright field optical microscope (OM) in reflection mode. (b) Impact zone observed in-situ using SIM based technique during structuring. (c) Impact observed ex-situ using a SEM technique.

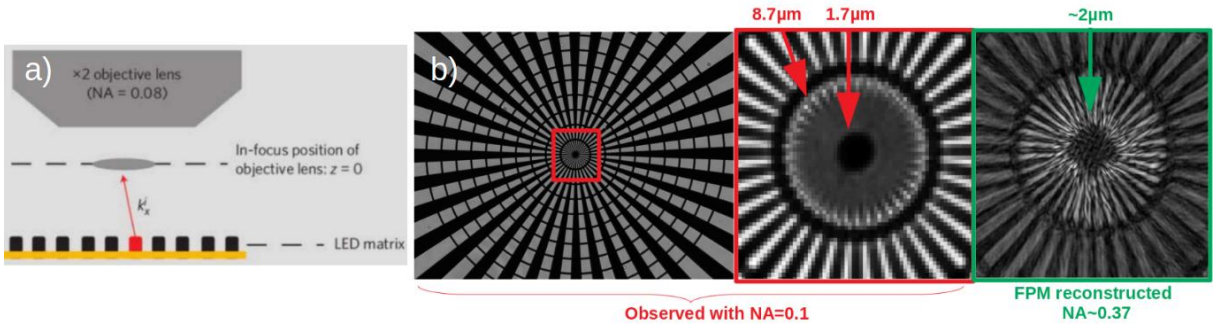

Fig. 3 a) Principle of FPM (adapted from [6]), b) Visualization of a sector target with FPM. Left: original image with low NA objective (0.1) showing a large field of view in the mm range. Center: detail of the original image center showing a 8.7 µm resolution because of the low NA objective. Right: Same area using the FPM reconstruction yielding a better resolution down to 2 µm

This opened the door to large field of view images acquired through an inexpensive low NA objective. The technique was first used for imaging biomedical samples, typically histological cuts. We discuss here the perspective of applying FPM to characterization of laser induced micro-nanostructuring of metallic surfaces.

The principle of FPM relies on a sequential illumination from multiple angle, usually achieved with an array of LEDs (see Fig. 3a)). Each angle of illumination corresponds to a specific zone of the Fourier space, in other words, high angles correspond to high spatial frequency regions in the Fourier domain.

By numerically recombining several angles using an iterative Fourier transform algorithm, a high resolution image can be reconstructed. As a proof of concept, we have performed the FPM technique on a transmission sector target as depicted on Fig. 3b). There, a four times increase in resolution could be achieved using the FPM technique, from 8.7 µm to 2 µm with a field of view in the mm range and a cm working distance. This proof of concept was achieved with a low cost standard LED array. The challenge is now to adapt the technique in reflexion and to push to submicrometric resolution in a reflective scheme.

4. CONCLUSION

Non-contact optical means are ideal tools for in-situ inspection of ultrafast laser induced surface micro and sub micro structures. In particular, we have shown that Structured Illumination Microscopy can offer a sufficient lateral resolution (155 nm) to precisely characterize LIPSS in-situ, enabling to follow the pulse to pulse pattern evolution. In order to expand the concept to larger field of view ond longer working distance, we explore the interest of Fourier Ptychography Microscopy. A proof of concept on a transmission resolution target has shown that 2 µm resolution could be reached experimentally with mm field of view and cm working distance. Further developments of FPM for in situ characterization of LIPSS include adaptation to reflective imaging and increase of the resolution power.

We thank the French ANR Labex Manutech-SISE funding (Sermonis and Ptycholaser).

REFERENCES

[1] P. Bizi-Bandoki, S. Benayoun, S. Valette, B. Beaugiraud, E. Audouard, "Modifications of Roughness and Wettability Properties of Metals Induced by Femtosecond Laser Treatment," Appl. Surf.e Sci. **257**, 5213-5218 (2011)

[2] B. Dusser, Z. Sagan, H. Soder, N. Faure, J. P. Colombier, M. Jourlin, E. Audouard, "Controlled Nanostructrures Formation by Ultra Fast Laser Pulses for Color Marking," Opt. Express **18**, 2913-2923 (2010)

[3] V. Dumas, A. Guignandon, L. Vico, C. Mauclair, X. Zapata, M. T. Linossier, W. Bouleftour, J. Granier, S. Peyroche, J. C. Dumas, H. Zahouani, A. Rattner, "Femtosecond Laser Nano/micro Patterning of Titanium Influences Mesenchymal Stem Cell Adhesion and Commitment," Biomed. Mater. **10**, 5 055002 (2015)

[4] A. Aguilar, C. Mauclair, N. Faure, J. P. Colombier, R. Stoian, "In-situ high-resolution visualization of laser-induced periodic nanostructures driven by optical feedback," Sci. Rep. **7** 16509 (2017)

[5] M. G. L. Gustafsson, "Surpassing the Lateral Resolution Limit by a Factor of Two Using Structured Illumination Microscopy". Journal of Microscopy **198**, nº 2 (1 mai 2000): 82‑87 (2000)

[6] G. Zheng, H. Roarke, Y. Changhuei, "Wide-field, high-resolution Fourier ptychographic microscopy," Nature photonics **7**, nº 9, 739‑45 (2013)

LIPSS NANOSTRUCTURING BY PICOSECOND LASER BEAM OF GDC/YSZ OXIDE THIN FILMS

W. KARIM[1*], A. PETIT[1], H. RABAT[1], M. TABBAL[2], A.-L. THOMANN[1], N. SEMMAR[1]

[1] GREMI-UMR 7344-CNRS-University of Orleans, 14 rue d'Issoudun, BP6744, 45071 Orleans Cedex2, France

[2] Department of Physics, American University of Beirut, Bliss St., P.O. Box: 11-0236, Beirut, Lebanon 1107 2020.

Corresponding author's E-mail: *wael.karim@univ-orleans.fr

Abstract

In ceramic solid oxide electrochemical cells (SOEC), a thin film of gadolinium-doped cerium oxide (GDC) is deposited (by plasma sputtering) between the electrolyte (yttrium-stabilized zirconia, YSZ) and the oxygen electrode (lanthanum-strontium-cobalt ferrite, LSCF) to reduce the formation of insulating phases at the electrode/electrolyte interface. In order to improve the adhesion between these layers as well as the ion exchange surfaces, we have considered a micro/nanoscale morphological structuring process using laser beams. The challenge is to successfully fabricate well-organized nanostructures, commonly referred to as LIPSS (Laser Induced Periodic Surface Structures), on complex oxide thin films such as GDC.

In this work, a Nd: YAG laser beam operating at the third harmonic (355 nm) with a relatively large laser beam spot (~500 μm) and emitting 40 ps laser pulses, is employed to irradiate a 2x2 cm^2 surface of 700 nm GDC thin layer under both static and scanning irradiation conditions. Using high resolution scanning electron microscopy (HR-SEM), it is found that LIPSS are produced at a low fluence laser multi-pulse regime close to the ablation threshold. In the static mode and under appropriate values of laser fluence F and number of pulses N, we have also identified two types of LSFLs that are distinct in their direction and spatial period. $LSFL_{//}$ are parallel to beam polarization, with a typical period of 238 nm and found in the center of the irradiated zone, whereas $LSFL_{\perp}$ are oriented perpendicular to beam polarization with a spatial period of 296 nm and found on the rim of the irradiated zone (Fig.1).

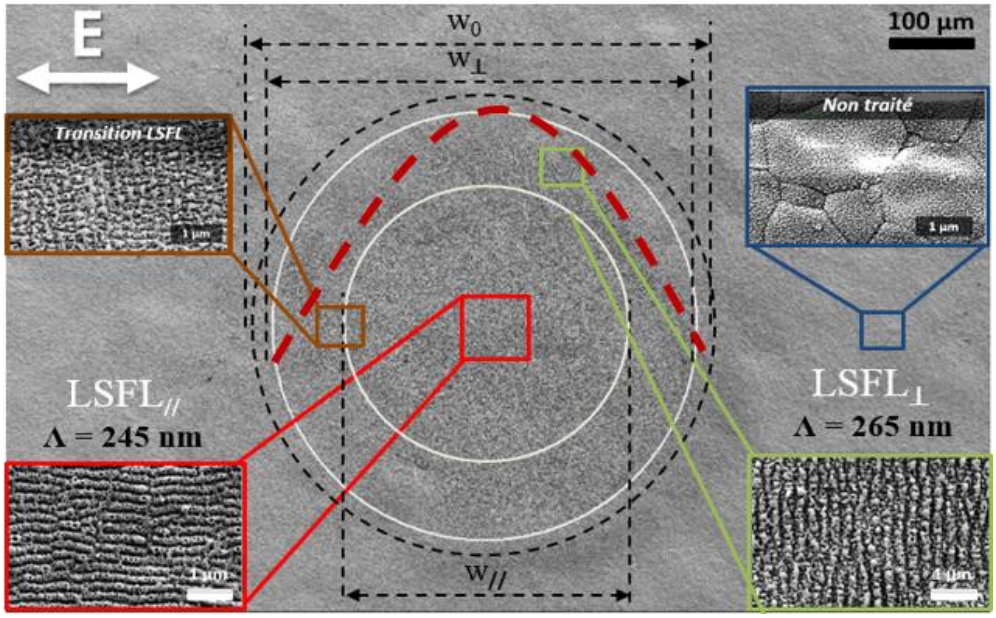

Fig.1: SEM image of the irradiated GDC film, for F=125 mJ/cm2 and N=10 pulses. The insets show the non-irradiated (untreated) surface as well as two different LIPSS patterns ($LSFL_{//}$ and $LSFL_{\perp}$) and the transition zone. W_0 is the beam spot size; $W_{\perp}$ and $W_{//}$ are the estimated diameters of $LSFL_{\perp}$ and $LSFL_{//}$ regions, respectively [1].

Our results suggest that the generation of parallel $LSFL_{//}$ is mainly attributed to a thermochemical process, while perpendicular $LSFL_{\perp}$ are due to a soft ablation process. A transition zone between these two types of LSFL manifested by the appearance of 'nano-squares' is due to the superposition of $LSFL_{//}$ and $LSFL_{\perp}$. We have also optimized the process parameters to generate well resolved LIPSS under beam scanning conditions.

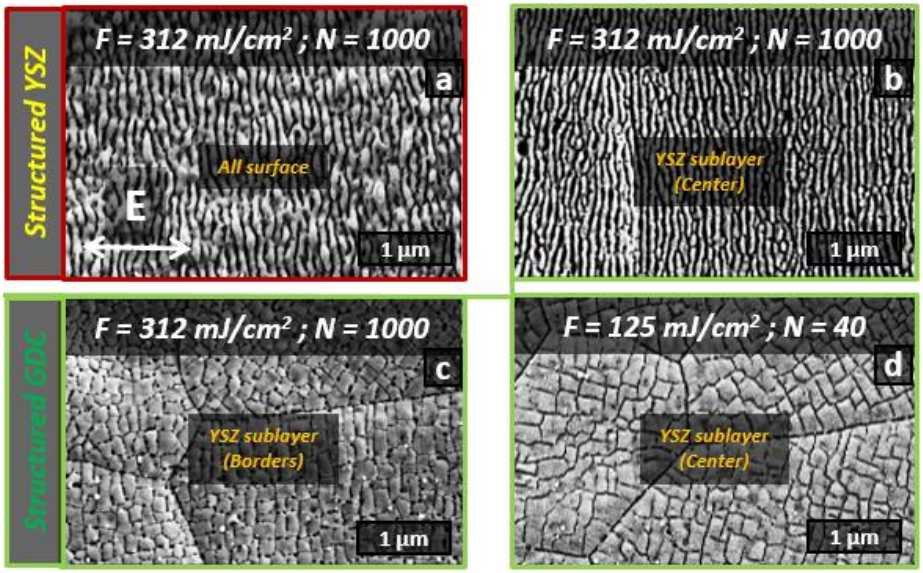

Fig.2: Comparison between the direct structuring of YSZ framed in red (a) and the structuring of YSZ functioning as the substrate of GDC thin film framed in green (b, c and d).

When ablation process of the GDC thin film takes place, the formation of organized patterns in form of square shaped cracks were observed on YSZ sublayer (Fig.2c-d). $LSFL_{\perp}$ were also identified on the YSZ surface, as well as HSFL (high spatial frequency LIPSS) formed on YSZ assisted by GDC thin film at a very large number of laser pulses (~1000) (Fig.2a).

The double scanning of laser beam in the same area of GDC with two different conditions (// and ⊥) leads to the formation of 2D structuring that were also obtained in scanning mode. Different surface characterization techniques (SEM-EDX, AFM, etc.), as well as COMSOL Mutliphysics simulations, have been used to interpret the obtained results. Considering the LIPSS sizes obtained in Fig.3 (better resolution of GDC cross section), with a geometric model, we were able to estimate a theoretical increase in developed area of 57% and 78% for 1D (regular LIPSS) and 2D periodic structures respectively. In this work, the largest experimental value reached is 42% for combined 2D structures of the 'nano-squares' type [1].

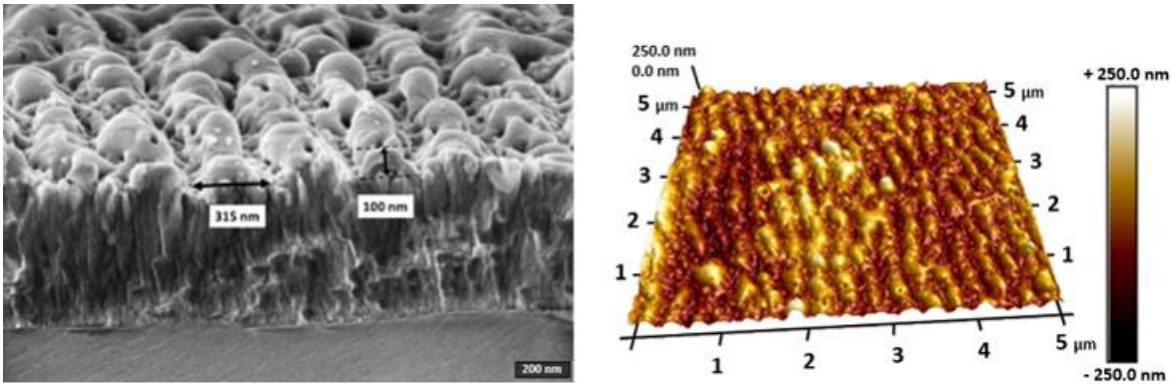

Fig.3: SEM cross section and 3D AFM images of 'nanosquared' surface of GDC/YSZ film for F=85 mJ/cm^2 [1].

REFERENCES

[1] Karim, W., Petit, A., Rabat, H. et al. Picosecond laser beam nanostructuring of GDC thin films : exchange surface enhancement by LIPSS.Appl. Phys. A 128, 731 (2022). https://doi.org/10.1007/s00339-022-05866-6

THE INFLUENCE OF LIPSS SPATIAL ALIGNMENT AND PERIODICITY ON OSTEOBLASTIC DIFFERENTIATION

X. SEDAO [1,2*], M. MAALOUF [3], A. A. KHALIL [1], Y. D. MAIO [2], S. PAPA [3], E. DALIX [3], S. PEYROCHE [3], A. GUIGNANDON [3] AND V. DUMAS [4]

[1] Hubert-Curien Laboratory, University of Lyon, Jean-Monnet University, UMR 5516 CNRS, F-42000 Saint-Etienne, France
[2] GIE Manutech-USD, 20 rue Benoît Lauras, F-42000 Saint-Etienne, France
[3] SAINBIOSE Laboratory INSERM U1509, University of Lyon, Jean Monnet University, F-42270 Saint Priest en Jarez, France
[4] University of Lyon, Ecole Centrale de Lyon, Ecole Nationale d'Ingénieurs de Saint Etienne, Laboratory of Tribology and Systems Dynamics, UMR 5513 CNRS, F-42100 Saint-Etienne, France

* xxx.sedao@univ-st-etienne.fr

ABSTRACT

Ultrashort pulse lasers have significant advantages over conventional continuous wave and long pulse lasers for texturing of metallic surfaces, especially for nanoscale surface structures patterning. Furthermore, ultrafast laser beam polarization allows precise control of the spatial alignment of the nanotextures imprinted on titanium-based implants surfaces. In this article, we report the biological effect of beam polarization on human mesenchymal stem cells differentiation. We created, on polished Titanium-6Aluminum-4Vanadium (Ti-6Al-4V) plates, Laser Induced Periodic Surface Structure (LIPSS) using linear or azimuthal polarization of Infra-Red beams to generate linear or radial LIPSS, respectively. The main difference between the two surfaces was the anisotropy of the Linear LIPSS and the isotropy of the Radial LIPSS. Seven days post-seeding, cells on the radial LIPSS surface showed the highest extracellular fibronectin production. At 14 days, qRT-PCR showed on the same surface an increase in osteogenesis-related genes such as alkaline phosphatase and osterix. At 21 days, mineralization clusters indicative of final osteoinduction were more abundant on the radial LIPSS. Taken together, we identify that creating more isotropic surfaces than linear enhances cell differentiation resulting in an improved osseointegration. Thus, fine tuning of ultrashort pulse lasers may be a promising new route for functionalization of medical implants.

1. INTRODUCTION

Titanium and related alloys, such as titanium-6aluminum-4vanadium (Ti-6Al-4V), have been used as the main biomaterial for dental and orthopaedic implant devices, which can be attributed to their resistance to corrosion, mechanical strength and high biocompatibility with host tissues. However, patients still face the risk of implant failure because of insufficient bone integration due to fibrous tissue production and/or the occurrence of infection. It remains a challenge to improve osseointegration with good mineralization at the bone–implant interface.

The femtosecond laser (FSL) offers the possibility to texture titanium at nanometric scales with controlled nanopatterns. Particularly, periodic nanostructures such as laser-induced periodic surface structures (LIPSS) are formed during a complex interplay between incoming laser light and surface waves. The periodicity of the LIPSS is closely linked to laser wavelength, and the direction of the LIPSS is determined by laser polarization. As a consequence, LIPSS with desired periodicity and linear or radial organization can be produced by applying FSL light with a well-defined laser wavelength and polarization. In the process of developing next-generation implants, it is of great importance to evaluate biological responses triggered by FSL-induced nanopatterns, which are dependent on surface parameters, including surface isotropy modification.

In this in vitro study, we assessed several stages of the osseointegration process. By providing aligned or disordered textures to the human Mesenchymal Stem Cells (hMSCs), we hypothesized that cells

differentially organize their focal adhesions and, more importantly, their fibrillar adhesion (increased cell contractility), thus accelerating their differentiation toward osteoblasts. Our results clearly indicate that isotropic texturing improved the induction of osteogenesis on titanium surfaces at all investigated time points.

2. EXPERIMENT DETAILS

Titanium samples were textured using FSLs from Amplitude Systems and galvo scanners from Scanlab within the GIE Manutech-USD platform (Saint-Etienne, France). The following laser sources were used: a Tangor HP and a Tangerine FSL (both from Amplitude Laser Groupe, Pessac, France), operating at 1030 nm central wavelength and a pulse duration of around 400 fs. Both lasers exhibited linear polarization states. All samples were placed on XYZ translation stages from Aerotech in order to find the best focusing plane. Scanlab GmbH's intelliSCAN 14 scanners were finally associated with f-theta lenses. Linear LIPSS (IR and GR, in some cases) and IR radial LIPSS were generated. In the later case an s-wave plate was implemented in the beam path of the laser to create a donut-shaped beam that converted the entering linear polarization into an azimuthal polarization.

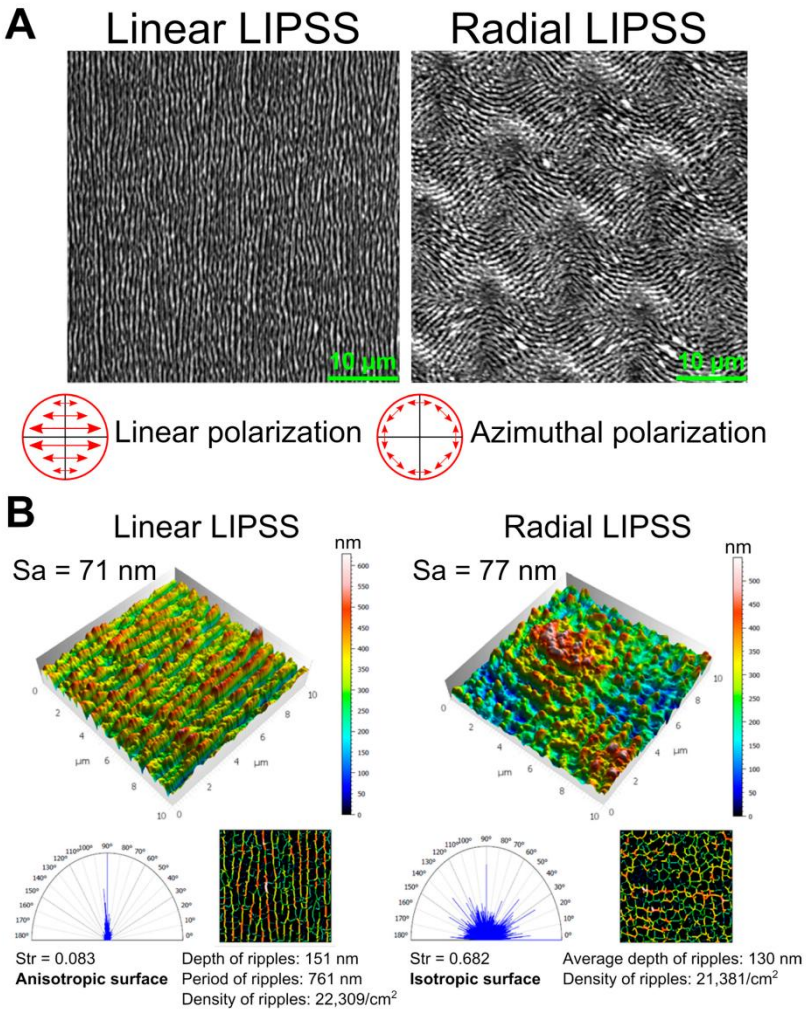

Fig 1. (A) SEM images of the two surface textures with linear or radial LIPSS (magnification 3000×). (B) 3D image reconstruction of the nanometer-scale surface texture with linear or radial LIPSS (data from atomic force microscopy images 10 µm × 10 µm) and surface analysis by Mountain Map® software.

3. RESULTS

The topography of titanium is one of the key features for the acceleration of osteogenic cell differentiation on medical implant devices. Stem cells interact with underlying surface patterns, which

lead to modulating the cell's fate. In this study, we focus our work on two different nanostructures obtained by FSL texturing. The nanoroughness of the two textures was similar, but one texture was anisotropic (linear LIPSS), whereas the other could be considered as isotropic (radial LIPSS). We demonstrate that isotropic texturing improves osteoblastic differentiation compared to anisotropic and polished surfaces. This was conducted by a cross-time investigation and by various operational techniques. Most dominant evidence is that at 21 days' post seeding, mineralization was assessed by calcein blue labelling. Image analysis revealed that hMSCs on the radial LIPSS surface had increased mineralization activity compared to the other two surfaces (Figure 2). This was highlighted by a larger mineralized area (+99% vs. polished, p = 0.016; +132% vs. linear LIPSS, p = 0.002) and a higher number of mineralized spots (+83% vs. polished, p = 0.046; +128% vs. linear LIPSS, p = 0.006) on the radial LIPSS surface. The average size of the mineralization spots was not different between the three surfaces.

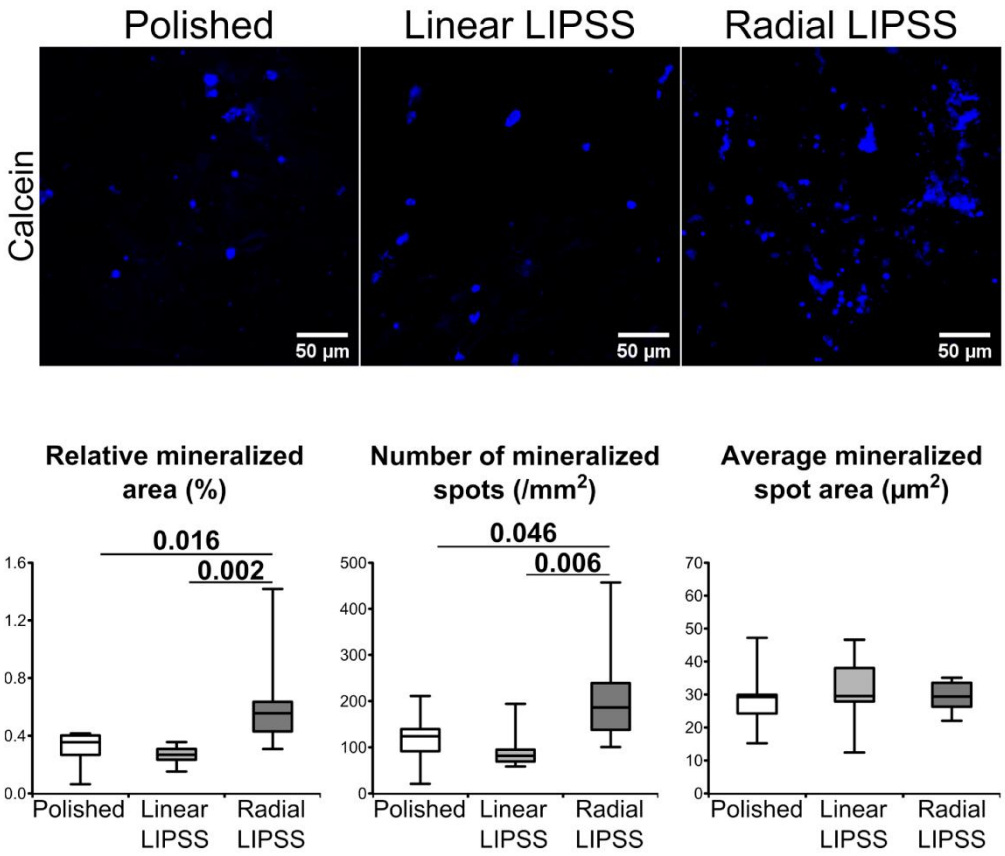

Fig. 2 Mineralization clusters labeled by calcein blue (blue) on the polished linear LIPSS and radial LIPSS surfaces at 21 d post seeding. On the bottom of the image are the results of the different quantifications made for the three surfaces.

This study provides insights into how small changes in laser polarization can modulate hMSC fate choice and extracellular matrix deposition. Nanoscale radial LIPSS generated on titanium alloys by FSLs with azimuthal polarizations exhibited an isotropic distribution that seemed to promote osteoblastic differentiation. Cell contractility and density, fibronectin production, gene overexpression and improved mineralization helped to ensure the consistency of cell evolution analysis over a time period of several weeks. Such dynamic hMSC sensitivity appears very important during implant osteogenesis, as these cells are primarily recruited to the implantation site. As a perspective, texturing titanium surfaces with such small features opens the possibility to couple-enhanced osseointegration with potential antibacterial properties, which are known to be more sensitive at the nanoscale than the microscale.

REFERENCES

[1] A. Klos, X. Sedao, T.E. Tatiana, *et al.*, " Ultrafast Laser Processing of Nanostructured Patterns for the Control of Cell Adhesion and Migration on Titanium Alloy", Nanomaterials **10**, 864 (2020).

[2] M. Maalouf, A.A. Khalil, and Y.D. Maio, *et al.*, "Polarization of Femtosecond Laser for Titanium Alloy Nanopatterning Influences Osteoblastic Differentiation" Nanomaterials **12**, 1619. (2022)

INDUSTRIALIZATION CONSIDERATIONS OF ULTRASHORT LIPSS TEXTURING FOR BIOLOGICAL APPLICATIONS

DI MAIO YOAN[1]*, AUBERT GUILLAUME[1], PASCALE-HAMRI ALINA[1], XXX SEDAO[1,2], MAALOUF MATHIEU[3], MUCK MARTINA[4], PALLARES-ALDEITURRIAGA DAVID[2], GRANIER JULIEN[1], PAPA STEVE[3], DUMAS VIRGINIE[5], GUIGNANDON ALAIN[3], HEITZ JOHANNES[4], COMPERE NICOLAS[1]

[1]GIE Manutech-USD, 20 rue Benoit Lauras, F-42000 Saint-Etienne
[2]University of Lyon, Jean Monnet University, Laboratory Hubert Curien, UMR 5516 CNRS, F-42000 Saint-Etienne
[3]University of Lyon, Jean Monnet University, INSERM U1059-SAINBIOSE, F-42270 Saint Priest en Jarez
[4]Institute of Applied Physics, Johannes Kepler University Linz, Altenberger Strasse 69, 4040 Linz, Austria
[5]University of Lyon, Lyon Central School, National School of Engineers of Saint-Etienne, Laboratory of Tribology and Systems Dynamics, UMR 5513 CNRS, F-42100 Saint-Etienne
*yoan.di-maio@manutech-usd.fr

ABSTRACT

In the context of the European H2020 Horizon project LaserImplant, we try to put in evidence that femtosecond laser texturing can play a key role by providing dedicated surface functionalization for biomedical implants [1]. Both osteoblast cell repellent surfaces [2] as well as surfaces promoting osteogenesis [3] are studied for two opposite applications: temporary bone screws and permanent dental screws. Two main texturing including LIPSS formation are proposed. This presentation will concentrate on industrial considerations as the end of the project aims at proposing a demonstrator to anticipate the commercialization of such processes. A versatile machine with limited processing times is expected and implies parameter upscaling that should avoid thermal effects and keep the surface properties developed by researchers at lower repetition rates. Dedicated beam delivery strategies are also studied and should adapt to different laser configurations depending on the textured products and their application.

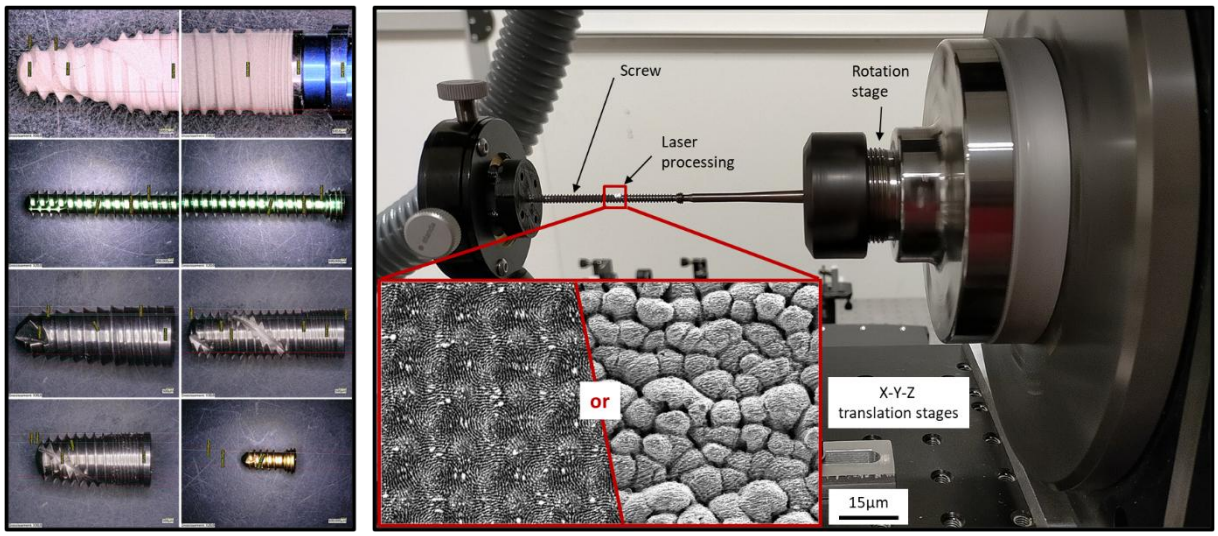

Fig. 1 : Left : Panel of considered screws to be textured during the LaserImplant project. Right : Example of a screw textured by laser with one of the two selected LIPSS pattern.

Titanium alloys (Ti6Al4V) are textured using several protocols and pattern designs with 1030nm ultrashort lasers. Different kind of polarizations associated with pre- or post-treatments reveal new surface functionalizations such as bone repellence or adhesion which are well suited for biomedical applications. The two promising textures selected by researchers are either composed of uniform spikes covered by LIPSS or tangential radial LIPSS. The choice of which texture to select mainly depends on the targeted product: permanent dental implant or temporary bone implant.

Industrial considerations concentrate on a unique laser solution that could easily provide both textures with acceptable processing times and quality robustness on screw type products with multiple dimensions. However each texture present specificities that are not necessarily compatible for a simple industrial workstation :

- Spikes covered by LIPSS require high recovering rates and are sensitive to thermal effects. Higher repetition rates as well as faster translation and rotation speeds are consequently limited, affecting the upscaling capacities. Playing with bigger beam diameters as well as a deeper look into parameter variations help improving such limitations.
- On the contrary, radial LIPSS are not drastically affected by repetition rates of several hundreds of kHz and marking speeds can be even faster due to a very low recovering rate. However, increasing the beam diameter to fit with spikes constraints may modify how bone cells interact with this surface.

These differences force to think about different beam delivery strategies but still compatible on a unique laser system. These strategies still have to be adapted to cylindrical parts with different lengths and diameters. Several mechanical constraints have to be also considered here such as limited rotation speed, translation speed, or time losses due to acceleration/deceleration of the moving parts. Previous to experimental tests thanks to a dedicated software, time simulators were developed to anticipate the pertinent configurations while showing their advantages and drawbacks.

Finally, post or pre-treatments are used to stabilize the surface functionalization provided by laser texturing. While spikes covered by LIPSS are coupled with post or pre-anodization as usually done for colored bone screws, dental screws do not present such treatments since most of the time sandblasted. For this last case, wettability tests on radial LIPSS are conducted since representative of the surface evolution in time. Different sterilization processes as well as storage environments are compared with unstructured surfaces to see the viability of such a technic for the industry.

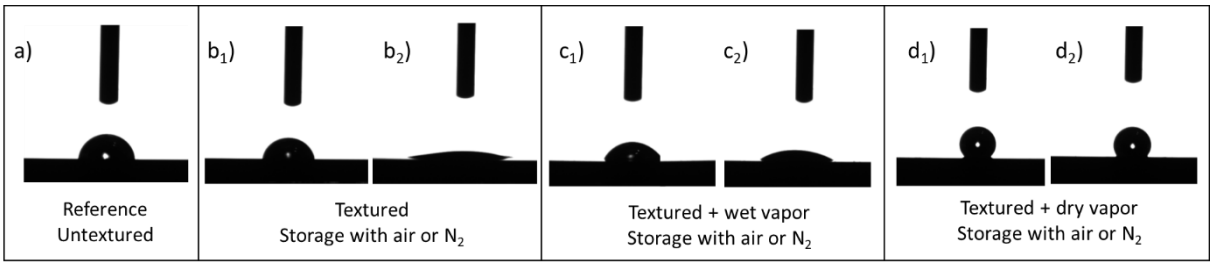

Fig. 2 : Differences of Titanium alloy wettability 11 days after laser texturing. Samples were not sterilized or sterilized by wet vapor (autoclave) or dry vapor (oven). Samples were stored in ambient air or in N_2.

REFERENCES

[1] https://www.jku.at/en/laserimplant/

[2] M. Muck, B. Wolfsjäger, K. Seibert, C. Maier, S.A. Lone, A.W. Hassel, W. Baumgartner, J. Heitz, “Femtosecond Laser-Processing of Pre-Anodized Ti-Based Bone Implants for Cell-Repellent Functionalization”, Nanomaterials 11, 1342 (2021)

[3] M. Maalouf, A. A. Khalil, Y. Di Maio, S. Papa, X. Sedao, E. Dalix, S. Peyroche, A. Guignandon, V. Dumas, "Polarization of femtosecond laser for titanium alloy nanopatterning influences osteoblastic differentiation", Nanomaterials, 1685223 (2022)

SMART LASER ENGRAVING SYSTEM FOR WIDE-BAND GAP MATERIALS FOR THE LUXURY INDUSTRY

ALEX CAPELLE[1,2], K. DEVA ARUN KUMAR[1], OLGA SHAVDINA[2]
BABACAR DIALLO[3], NADIA PELLERIN[3], BARTHÉLEMY ASPE[1], LÉO THOMAS[1],
MARTIN DEPARDIEU[2], ANNE-LISE THOMANN[1], NADJIB SEMMAR[1*]

[1]GREMI - CNRS UMR 7344, Orléans, France
[2] Décor World Services (DWS), Orléans, France
[3] CEMHTI - CNRS UPR 3079, Orléans, France, as collaborator from ARD MATEX
corresponding author: nadjib.semmar@univ-orleans.fr

ABSTRACT

The decoration of glass has become a major issue for manufacturers of packaging for cosmetics, perfumes or wines and spirits, particularly represented in the CVL Region. These manufacturers use many processes aimed at coloring and texturing the glass on the surface or in volume. Laser stripping process makes it a promising way to obtain a certain surface texturing offering a particular decorative aspect, while laser engraving makes it possible to print very fine patterns on both the surface and volume of the glass.

1. INTRODUCTION

This project aims to master light-matter interaction between common lasers and products from the luxury industry which represent scientific interests. A novative approach using machine learning algorithm and computer vision will be developed and implemented.
Obtaining a specific and reproductible visual texture is very important in the luxury sector and finding the right set of parameters (laser beam and stage moving) to obtain the desired rendering is often a time-consuming process. It requires a good knowledge of the laser engraving system (engineer work), experience in searching for a desired rendering (artisanal work) which will satisfy customers expectations (artistic work).
In this scope, machine learning algorithm seems to be a convenient tool to link a set of visual characteristics with the agreement of a customer. The visual characteristics are obtained by a set of measurement techniques (characterisation system). The study of light-matter interaction mechanisms will be the link between laser beam characteristics and surface texture characteristics.
This final goal will be achieved by first replacing the customer by a characterization system composed of physical measurements combined with optimisation criteria. Moreover, the training of the algorithm requires a certain quantity of data for learning and testing. The characterization system will then be developed to generate the required quantity of data in a reasonable time.

Fig. 1 Decorated glass (DWS)

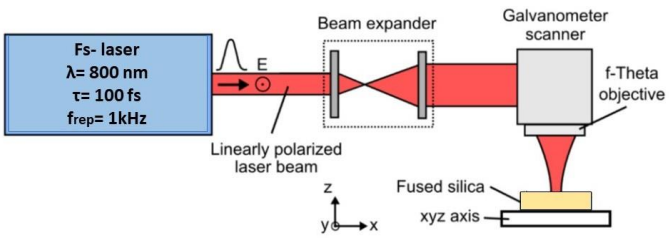

Fig. 2 Scheme of the experimental setup used for the generation of laser-induced periodic surface structures (LIPSS) on fused silica

The first step of this work will be to selected one material and study the mechanisms with three industrial lasers. The material of study will be industrial soda-lime container bottles and the selected lasers are microsecond NIR CO_2 laser, Picosecond UV Ti:sapphire, Femtosecond IR Ti:sapphire.
The second step will be to list the mechanisms, for example direct scribing, LIPSS, defragmentation, melting, suitable for creating interesting visual textures. Here, Laser-induced periodic surface structures (LIPSS) are a universal phenomenon that can allow tailoring nano-electronics and nano-photonics devices. The generation of LIPSS in a single-process step provides a simple way of surface nanostructuring toward a control of optical, mechanical, or chemical surface properties, which can be used for various applications [1]. Several experimental parameters have been identified to be important for the generation and control of LIPSS. Apart from the laser wavelength and the laser beam polarization, two important key parameters are the laser fluence ϕ (energy density in J/cm^2) and the number of laser pulses N applied to the same spot. Moreover, the angle of incidence θ affects the LIPSS periods as well as the local environment. While the periods of LIPSS generated in air and vacuum are quite similar, the irradiation in liquids usually leads to a significant reduction of the LIPSS periods to values as small as ~100 nm [2].

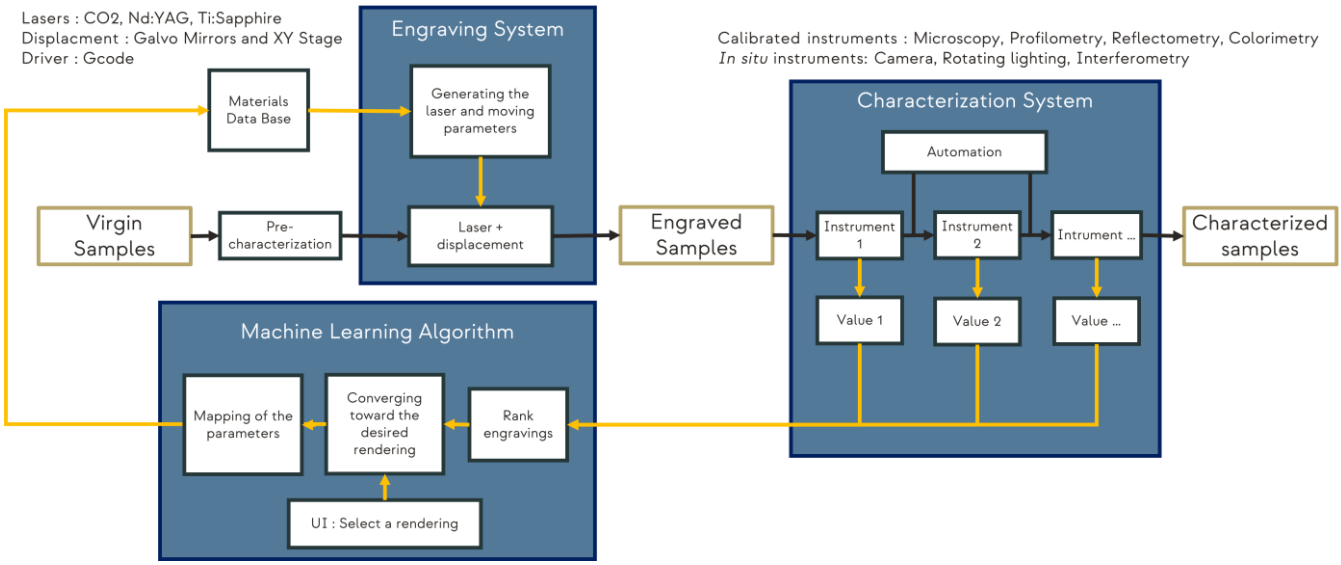

Fig. 3 Smart system diagram

However, for commercial applications, processing in air is strongly desirable in order to avoid expensive equipment with vacuum and reducing the working time and the production costs. In this aid, the current research state in this field of LIPSS generated by fs-laser pulses in air.
In order to study the impact of transient changes of the optical properties of LIPSS formation, we have to choose the dielectric material since a large difference between the optical properties of nonexcited (dielectric) and the strongly fs-laser pulse excited (metal like) material can be expected. Therefore, the main work will be to study the mechanisms of femtosecond lasers with glass surfaces (soda-lime container bottles). Followed by the generation of LIPSS on glass surfaces will be studied using a femtosecond laser. The laser-irradiated surface regions will be characterized by optical microscope (OM) and scanning electron microscopy (SEM).
The third step will be to use the characterization system to maximize the visibility criteria, which will be detailed in the presentation and process characteristics like average depth of modification, process time, residual stress…
Finally, all of these criteria will be input in the machine-learning algorithm, which will attempt to match them with human feeling rating.

REFERENCES

[1] J. Bonse, J. Krüger, S. Höhm, et al. J. Laser Appl. 24, 042006 (2012)
[2] C. Wang, H. Huo, M. Johnson, M. Shen, and E. Mazur, et al. Nanotechnology 21, 075304-1–5 (2010)

Author index

Wednesday, September 21

11:00	Welcome	
12:30	Lunch	
14:00	Welcome talk	**Anne-Lise Thomann** GREMI, Orléans
14:10	Presentation of Le Studium	**Aurélien Montagu & Marie Artiges** Le Studium, Orléans
14:30	Introduction to the LIPSS Workshop	**Jurgen Reif** BTU, Cottbus-Senftenberg
15:00	Formation dynamics of periodic surface patterns in Ge induced by UV nanosecond laser pulses	**Jan Siegel** Instituto de Optica-CSIC, Madrid
15:35	Coffee Break	
15:55	How the combination of electromagnetic effects and thermophysical properties of solids influences the formation of laser induced periodic surface structures	**George Tsibidis** IESL-FORTH, Heraklion
16:30	Bio-inspired laser micro- and nanopatterning for fluid transport and anti-adhesive properties	**Cristina Plamadeala** Johannes Kepler Universität, Linz
17:05	Round table	
17:45	End of working day	
18:00	Visit of old town	

Thusrday, September 22

09:00	LIPSS formation on polymer thin films: influence of thickness, roughness and substrate	**Esther Rebollar** IQFR-CSIC, Madrid
09:35	LIPSS with extreme properties: short period and high aspect ratio	**Evgeny Gurevich** University of Applied Science, Münster
10:10	Coffee Break	
10:30	Surface Morphology at Nanometric Scale by Temporal and Polarization Control of Ultrashort Laser Pulses	**Anthony Nakhoul** Laboratoire Hubert Curien, Saint-Étienne
11:05	Stochasticity versus determinism in LIPSS formation	**Jean Philippe Colombier** Laboratoire Hubert Curien, Saint-Étienne
11:40	Investigation of LIPSS structures fabricated in different surrounding media using focused-ion beam etching	**Matej Senegacnik** Faculty of Mechanical Engineering, Ljubljana
12:15	Lunch	
14:00	Round table	
14:30	Significance of laser processing environments in determining the surface chemistry, ageing and final response of HSFLs generated on Tungsten	**Priya Dominic** Laboratoire Hubert Curien, Saint-Étienne
15:05	Microscopy techniques for in-situ LIPSS detection and characterization via optical means	**Cyril Mauclair** Laboratoire Hubert Curien, Saint-Étienne
15:40	LIPSS nanostructuring by picosecond laser beam of GDC/YSZ oxide thin films	**Wael Karim** GREMI, Orléans
16:15	Coffee Break	
16:35	Sponsors' presentations	**Opton Laser, Amplitude, Optoprim**
17:35	End of working day	
19:00	Gala dinner at Bateau Lavoir	

Friday, September 23

09:00	Mitigation of secondary electron yield by femtosecond pulse laser-induced periodic surface structuring	**Salvatore Amoruso** Complesso Universitario di Monte S. Angel, Napoli
09:35	The influence of LIPSS spatial alignment and periodicity on osteoblastic differentiation	**Xxx Sedao** Laboratoire Hubert Curien, Saint-Étienne
10:10	Coffee Break	
10:30	Industrialization considerations of ultrashort LIPSS texturing for biological applications	**Yoan Di Maio** GIE Manutech-USD, Saint-Étienne
11:05	Smart laser engraving system for wide-band gap materials for the luxury industry	**Alex Capelle** GREMI, Orléans
11:40	Round table	
12:10	Closing session - Conclusions - Next workshop organization	
12:30	Lunch	
14:00	Potential visit: GREMI laboratory and DWS start-up	
17:00	End of working day	